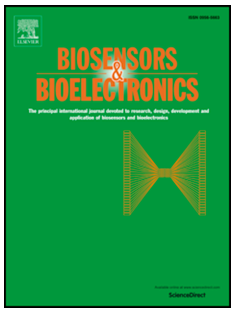

Strategies to improve performances of LSPR biosensing: Structure, materials, and interface modification

Tianping Xu, Zhaoxin Geng

PII: S0956-5663(20)30836-8

DOI: https://doi.org/10.1016/j.bios.2020.112850

Reference: BIOS 112850

To appear in: *Biosensors and Bioelectronics*

Received Date: 24 August 2020

Revised Date: 6 November 2020

Accepted Date: 22 November 2020

Please cite this article as: Xu, T., Geng, Z., Strategies to improve performances of LSPR biosensing: Structure, materials, and interface modification, *Biosensors and Bioelectronics* (2020), doi: https://doi.org/10.1016/j.bios.2020.112850.

Strategies to Improve Performances of LSPR Biosensing: Structure, Materials, and Interface Modification

Tianping Xu[a] and Zhaoxin Geng[a, b*]

[a] School of Information Engineering, Minzu University of China, Beijing, 100081, P. R. China
[b] State Key Laboratory for Integrated Optoelectronics, Institute of Semiconductors, Chinese Academy of Sciences, Beijing, 100083, P. R. China

*Corresponding author.
E-mail addresses: zxgeng@muc.edu.cn (Z. Geng).

ABSTRACT

Due to the unique nature of localized surface plasmon resonance (LSPR), LSPR has attracted extensive attention in the field of biochemical sensing. However, compared with other sensors, the LSPR biosensor has lower sensitivity which has the limitation of insufficient repeatability and greatly limits its application and further promotion. Many researchers have invested a lot of energy in various ways to investigate different methods to improve sensitivity. This review summarizes these methods from the three aspects of structure, material, and interface modification, LSPR signal observation. Meanwhile, it can be predicted that strategies to improve the performance of LSPR biosensing.

A R T I C L E I N F O

Key words:

Localized Surface Plasmon Resonance; Biosensor; Sensitivity; Plasmonics.

1. Introduction

Biosensors have always played an important role in medical diagnosis and environmental monitoring (Chao et al., 2016; Mehrotra, 2016; Rissin, n.d.). Among them, plasmonic-based sensors have received widespread attention for their excellent performances because the evanescent wave has an enhanced electric field in the penetration depth and is extremely sensitive to the changes in the refractive index of the medium. Therefore, plasmonic-based sensors also are typically sensed by amplifying the signal of the target analyte, such as plasmonic-enhanced fluorescence (PEF) (Bauch et al., 2014; L. Wang et al., 2015), surface-enhanced Raman scattering (SERS) (Campion and Kambhampati, 1998; Fleischmann et al., n.d.; Langer et al., 2020), surface-enhanced infrared absorption (SEIRA) (Leidner et al., 2016), and plasmonic-based colorimetric analysis (Tang and Li, 2017); biosensing can also be performed by detecting changes in the relevant frequency of the surface plasmon resonance in the presence of the target analyte, such as surface plasmon resonance (SPR) biosensors (Lesuffleur et al., 2007; Liu et al., n.d.) and localized plasmon resonance (LSPR) biosensors (Chuang et al., 2015; Takei et al., 2014).

Relatively speaking, SPR and LSPR systems were put into commercial use earlier (Oliverio et al., 2017a).

Broadly speaking, the detection limit of SPR biosensor is insufficient due to surface plasmon polaritons (SPP) requires prism or grating coupling and the detection depth is greater than 200nm which is bulk effect detection (Chen, 2012). It is difficult to quickly analyze and detect micro-molecule with low concentrations, which hinders it to keep up with the trend of miniaturization, convenience, and integration of end-to-use equipment. Comparing with the working principle of LSPR and SPR, LSPR biosensors seem to match these new trends better. The corresponding equipment of LSPR is small in size, which could be easily integrated. Therefore, different LSPR biosensors or testing setups were developed for different application fields, especially for the detection of small molecules and very low concentration samples (Chien et al., 2018; Nunna, 2019; Sagle et al., 2011; Willets and Van Duyne, 2007). Since the LSPR frequency depends on the size, shape, interparticle spacing, and dielectric properties of the material, as well as the dielectric properties of the local environment that surrounds the nanostructures, which can work flexibly in a wide spectral range (Chen et al., 2018; Langer et al., 2015). However, with the development of related disciplines and the needs of early diagnosis for major diseases, the requirements for measurement accuracy of LSPR biosensor have become higher and higher. Many results on LSPR sensing technology have shown that traditional LSPR biosensors have exposed some shortcomings, such as small resonance peak (valley) shift, insufficient resonance strength, wide linewidth characteristics, small peak-to-valley ratio, and so on (Chen et al., 2011a; Liang et al., 2017), which limit its application in high precision detection of the biochemical sensor. For example, a single protein molecule in an aqueous solution could only cause LSPR resonance peak shifts below 0.1 nm on average (Chen et al., 2011a). If the signal amplification mechanism is not introduced, the LSPR peak shift caused by the binding of the molecule to the metal-nanostructure substrate is usually less than 1 nm (Chuang et al., 2015). Compared with SPR biosensing using SPP on a metal film, the sensitivity of LSPR biosensing is at least one order of that of SPR biosensing (Chen et al., 2018). Therefore, to improve the sensitivity of the LSPR biosensor is an urgent requirement for the detection of very low concentrations of samples or early detection of biomarkers of key diseases.

LSPR is an optical phenomenon generated by a light wave trapped within conductive nanoparticles (NPs) smaller than the wavelength of light. The phenomenon is a result of the interactions between the incident light and surface electrons in a conduction band. The noble metal nanostructure absorbs photon energy to produce obvious extinction characteristics and near-field enhancement characteristics. The extinction spectrum of the noble metal nanostructure would peak when the LSPR is excited. The wavelength corresponding to the peak is called the resonance wavelength (λ_{max}), and how many peaks depend on the size of the nanostructure and resonant mode. The resonance wavelength is sensitive to the refractive index change at the interface between the nanostructure and surrounding media when LSPR occurs.

In general, if the refractive index of the surrounding medium increases, the extinction spectrum redshift and the resonance wavelength increase. The opposite can also happen if the refractive index of the surrounding medium decreases. This phenomenon means that the LSPR extinction (or scattering) wavelength maximum, λ_{max}, is sensitive to the dielectric constant ε (or refractive index, n; both are related by $\varepsilon = n^2$). The wavelength-shift at λ_{max} is given by equation (Jung et al., 1998):$\Delta\lambda_{max} \cong m(\Delta n)[1 - \exp(-2h/I_h)$. Here m is the bulk refractive-index response of the

nanostructures; Δn is the change in the environmental refractive index; h is the effective adsorbate layer thickness; I_h is the electromagnetic field decay length (approximated as an exponential decay). This feature is the basis of the LSPR biosensor for sensing measurements. The LSPR shift induced by the adsorbates, $\Delta\lambda_{max}$ was rewritten as $\Delta\lambda_{max} = \Delta\lambda_{max}(after) - \Delta\lambda_{max}(before)$. Therefore, LSPR can become an ideal refractive index sensing platform. This kind of refractive index sensing depends on the shift of the resonance peak. Therefore, to judge the sensing performance of this sensor needs to start from the spectrum, and also needs to have corresponding parameters to judge. The main parameters for evaluating the sensing performance of LSPR sensors are sensitivity.

Sensitivity (S) is determined by the offset of the resonance wavelength ($\Delta\lambda$) and the variation of the refractive index (Δn) at the interface, defined as the ratio of the offset of the resonance wavelength to the variation of the ambient refractive index (Chung et al., 2011): $S = \Delta\lambda/\Delta n$. Where the unit of $\Delta\lambda$ is the nm; the unit of Δn is the RIU; the unit of S is the nm/RIU (nanometers of peak shift per refractive index unit).

The LSPR sensing precision that can be achieved concerning changes in the refractive index depends on the sensitivity, S, and the peak line width. The size of the nanostructure affects the sensitivity and peak line width. For example, larger nanoparticles tend to have high sensitivities, but their peaks are broadened by multipolar excitations and radiative damping. A figure of merit (FOM) is determined by the sensitivity and the resonance line width (d, the unit: nm), defined as the ratio of sensitivity to resonance line width (Chung et al., 2011), $FOM = S/d$, which is widely used to characterize the sensing capabilities of LSPR biosensor.

In the actual biochemical sensor detection, it also involves a more important indicator: the limit of detection (LOD). The LOD is defined as the smallest detectable signal (spectral change) caused by the interaction of the detected analyte (Homola, n.d.). By definition, this indicator has two determinants: one is the size of the spectral change caused by analyte interaction, and the other is the resolution of the detection spectrum of the device. The former is the sensitivity and FOM introduced above and the latter, resolution (also called the minimum resolution), is usually defined as the minimum detection limit of the sensing instrument.

To improve the performance of LSPR biosensor, it is necessary to cooperate in many aspects such as structure design, sensitizing materials, surface modification of sensor elements, to satisfy the sensing detection of extremely low concentration samples. Although there are many works on LSPR sensing technology, the methods of LSPR enhance-technology have not been systematically summarized in essence. Therefore, this paper would summarize the methods of the LSPR sensitization technique from the following aspects.

Firstly, we reviewed the method of changing the nanostructure to increase sensitivity and how to affect the performances of LSPR biosensors. Secondly, the effect of changing biosensor materials on sensitivity, especially metamaterials and two-dimensional materials, was presented, summarized, and compared. Thirdly, the method of increasing sensitivity from modification at the interface between nanostructures and environmental media were reviewed and summarized. Finally, the processing method of the LSPR biosensor signal is described. Meanwhile, the methods to enhance sensitivity and research direction are also presented.

2. Strategy to Enhance the Performance of LSPR biosensor

2.1. Enhance performance by change nanostructure to create hot-spot

2.1.1. Changing nanoparticle shape in disorder or single

The sensitivity of the biosensor based on LSPR is directly related to the local electric field intensity of the nanoparticles, which is positively correlated with the intensity of the local electric field. Nanoparticles with different shapes produce different local electric field intensities when light excited LSPR. Spherical nanoparticles with their extreme symmetry characteristics would present uniform electric field distribution, in other words, there is no obvious “hot spot”, which result in low sensitivity of the LSPR biosensor. If increasing the aspect ratio of the nanoparticles and breaking the symmetry of the nanoparticles, the electric field enhancement improves effectively (Chung et al., 2011). Therefore, it is feasible to increase the sensitivity of the sensor by changing the shape of the nanoparticles, such as nano-crescent shape(Lu et al., 2005; Shumaker-Parry et al., 2005), nano-triangle(Jensen et al., 1999; Sherry et al., 2006), spherical shell (Averitt et al., 1997; Hirsch et al., 2003; Sun and Xia, 2002; Tam et al., 2004), nanodisk(Dahlin et al., 2009; Haes and Van Duyne, 2002), nanostar (Nehl et al., 2006), nanohole (Escobedo, 2013; Prikulis et al., 2004; Rindzevicius et al., 2005), etc. For example, in 2019, Hangsong et al. proved experimentally that the local electric field intensity of triangle silver nanoparticles is 10 times stronger than that of spherical silver nanoparticles. The extinction efficiency of triangle silver nanoparticles is 4 times bigger than that of spherical silver nanoparticles (Song et al., 2019). This is due to the three angles are "sharper" than that of the sphere. According to the principle of tip discharge, the surrounding electrons would gather near the tip, which makes the electric field stronger at the protruding point. If nano-triangle particles are thinner, the electrons distribute on the edge of the nano-triangle particles. When the polarization direction of the incident light is parallel to the edge of the nano-triangle particles, the electric field intensity on the surface is greater than that of other cases. Meanwhile, the light absorption at the resonance wavelength is also stronger. The experiment results illustrate that triangular nanostructures (less than 100nm in size) can generate strong electric fields and are relatively sensitive, however, this is highly dependent on the direction of polarized light. If a large number of triangular nanostructures are arranged in order, the sensitivity is relatively high. The full-width at half-maxima (FWHM) would be significantly increased. Therefore, it is necessary to implement LSPR sensing by using triangular nanoseconds: 1) Triangular nanoseconds should be arranged orderly with uniform and uniform structure; 2) The size is less than 100nm, and the distance among nanostructures is less than 100nm; 3) The polarization direction of the incident light should be parallel to one side of the triangle; 4) The metal thickness is less than 100nm. The challenge lies in the high cost of nanostructure fabrication and the difficulty of large-area preparation.

For rapid and low-cost fabrication, chemosynthetic methods are widely used to fabricate nanostructures, for example, nanorice structures. Nanorice structure consists of nanorod and nanoshell (Wang et al., 2006). The material of the innermost nanorod is iron oxide. The material of the outside nanoshell is a thin gold film. Nanorice structures exhibit a strong local field enhancement which can also be tuned. The sensitivity based on longitudinal and transverse plasmas is 801.4 nm/RIU and 103.0 nm/RIU, respectively, which is very attractive for surface enhancement spectra or highly sensitive measurements. Experiments show that the sensitivity is higher when the polarization of incident light is consistent with the length direction of nanorice, which is not convenient in the use process. Therefore, higher requirements are put forward for the detection scheme.

Nanostructure pairs can effectively modulate electromagnetic field distribution to achieve

higher sensitivity. For example, in 2015, Hu et al. studied two heterodimers with different materials of the same size (Hu et al., 2015). They found that Au-Ag nanometer rice-type dimers have a good optical response: Fano resonance has an “enhancement” effect for the circular dichroism (CD). During the change of the surrounding refractive index from 1.1 to 1.4, the heterodimer shown FOM values up to 21.6 due to Fano assisting the CD. This kind of method can realize light field regulation by changing the spacing between materials and nanostructures, to achieve a higher LSPR sensing technology. However, due to the high cost, it cannot be widely used in the field of biochemical sensing.

Au-nanostar (AuNS) is also a typical nanostructure that can effectively improve the sensitivity of the LSPR sensor. Au nanostar particle has multiple sharp corners that can produce the “hot spot” of the electric field. Therefore, when the refractive index of the medium changes, the extinction spectra of the nanostar shift tremendously. It has been reported that AuNS exhibited 5 times higher sensitivity than that of sphere particles (Yuan et al., 2013). Park et al. proposed AuNS clusters formed by self-assembly of affinity ligands based on AuNS particles (Park et al., 2015). Firstly, the experimenters proved that AuNS exhibited superior refractive index sensitivity and higher FOM value than AuNP. Secondly, the AuNS dimer was simulated. AuNS dimers are a simplified form of clusters. The results showed that the energy density of this dimer was 460 times higher than that of the gold nanosphere dimer. And the spectral shift produced by binding to the ligand was significantly larger than the spectral shift produced by binding of a single gold nanostar particle to the ligand. It can be concluded that this structure has great application potential in biosensing.

If the angle between the spherical nanoparticles and the substrate is continuously increased by fine-tuning the particle shape, the particle shape would slowly transition from a spherical shape to a disc shape. If the included angle is less than 90°, the smaller the angle, the closer the shape is to a spherical shape; if the included angle is greater than 90°, the larger the angle, the closer the shape is to a disc (Chung et al., 2019). The shape of the disc and the shape changed on this basis have also attracted the attention of many researchers. E. Hanarp et al. introduced the flat nanodisk structure and compared it with the ordinary nanodisk, pointing out that increasing the aspect ratio can improve the sensitivity of the particle extinction spectrum to the change of the refractive index in the external environment (Hanarp et al., 2003). Ai et al. also improved the sensitivity of the sensor by changing the aspect ratio of the structure. They proposed an elliptical hole based on the circular hole (Ai et al., 2017). Incident polarized light had different transmission spectrums in the long and short axis directions of this structure. Because a highly confined electric field is generated on the metal surface, SPR is more sensitive to the changes in the surrounding refractive index that it can produce a larger response. The results showed that the elliptical nanohole-based plasma sensor had a sensitivity of 775 nm/RIU and a FOM value as high as 705 RIU^{-1}. Changing the aspect ratio introduces asymmetry. Here the asymmetry is combined with changing the particle shape. Compared to the previous introduction, which only changed the shape of the particles to other symmetrical shapes, the sensitivity was improved again. This is a simple and effective way to increase sensitivity.

Chung et al. introduced in the article a nano-crescent structure with large field enhancement at the tip of the structure(Chung et al., 2011). While the location where there is local field enhancement is usually called “hot-spot”, molecular sensing at the hot spot can provide high sensitivity. Generally speaking, most nano-crescent structures are prepared by physical methods.

Among them, it is still very challenging to synthesize an asymmetric structure like a crescent in the solution phase. Although this structure does not adopt the method of changing the aspect ratio, it also introduces asymmetry. And to some extent, its asymmetry is more obvious.

Throughout the years of research on the shape of particles to affect the sensitivity of LSPR sensor, there are clear trends in the shape of the particles under study. In the beginning, the spherical nanoparticle was replaced with other three-dimensional shapes for adding the "tip". Then, on the basis of adding the "tip", there are two trends: One was to change the aspect ratio of the particles that the symmetry of the particles was changed limitedly; another is to change the positional distribution of part of the particle structure that the symmetry of the particles was changed greatly. Here present a few simple shapes as an example, as shown in Figure 1. The comparison of different nanostructures LSPR sensors with different shapes also presented in Table 1.

The size of the particle also affects the sensing performance of the sensor to a certain extent by affecting the resonance peak shape. Take a spherical particle as an example. When the particle size is small, it can be regarded as a pair of dipoles. Dipole resonance is the main cause of plasmon resonance at this time, so the cross-section of light absorption (the volume of the particle) is proportional to the resonance intensity. However, when the diameter of the particles is greater than 60 nm, the retardation effect and the contribution from higher vibration modes would cause the resonant peak to broaden (Yockell-Lelièvre et al., 2015), making the FOM smaller and affecting the sensing performance.

Table 1: The comparison of different nanoparticle LSPR sensors of different shapes.

Author	Name	Shape	Material	Sensitivity	Ref.
Helene, et al.	Sphere		Au	83 nm/RIU FOM: 1.3	(Yockell-Lelièvre et al., 2015)
Hang, et al.	Triangle		Ag	1116.8 nm/RIU	(Song et al., 2019)
Wang, et al.	Rice		Au, Fe_2O_3	801.4nm/RIU	(Wang et al., 2006)
Hu, et al.	Double-rice		Au	FOM: 21.6	(Hu et al., 2015)
Park, et al.	Star		Au	250-500nm/RIU	(Park et al., 2015)
Ai, et al.	elliptical hole		Ag	775nm/RIU	(Ai et al., 2017)
Jang, et al.	Crescent		Au	-	(Chung et al., 2011)

No matter which nanostructure is used, if the nanostructure is arranged in a disordered manner and the distance between the nanostructures is far beyond the resonance wavelength, the transmission or reflection spectrum would be broadened, the FWHM would be larger, and the spectral shift with the refractive index would be small, which is essentially the average effect of the transmission or reflection spectrum of each nanostructure. As a result, the resonance wavelength shifts small and repeatability is poor, which makes it difficult to get the real clinical application. Therefore, the disordered nanostructures are utilized as spectral-resolved

single-particle detection (SPD) methods for biological analysis and disease diagnosis. Single-particle acts as a signal probe and each particle are considered as an independent signal output, which can e□ectively avoid the interference of the ensemble averaging e□ect and improve spatiotemporal resolution, which makes it possible to sensitively detect sample at a single-particle (or-molecule) level under a dark-field microscope (DFM). Up to now, many single plasmonic resonant nanoprobes have been developed and employed in the DFM-based SPD assay because of their prominent optical properties originated from LSPR such as a silver nanoparticle, gold nanorod, gold nanoparticle (AuNP), gold prism, and gold nano-flower. DFM-based SPD assay can combine spectroscopy and fluorescence to greatly improve the accuracy of each test, and the analysis method of a single nanostructure can make sample consumption very small. However, in the detection of biochemical sensing, the spectrum needs to be measured several times. In the case that in-situ detection is not possible, it is difficult to accurately determine that multiple measurements before and after the measurement are for the same nanostructure, which requires high requirements for accurate positioning and nanostructure identification, and it is also difficult to achieve. Therefore, this method can be used in the laboratory, but it is difficult to be widely used in clinical practice, or it is difficult to use the detection results of single nanostructure LSPR technology as a criterion for clinical application.

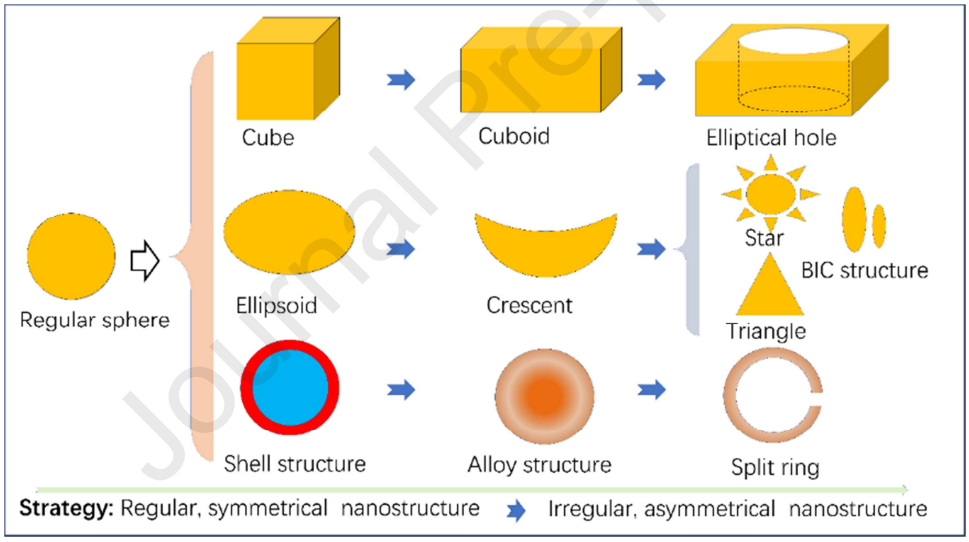

Figure 1. Strategy to change nanostructure shape for enhancing the performance of LSPR.

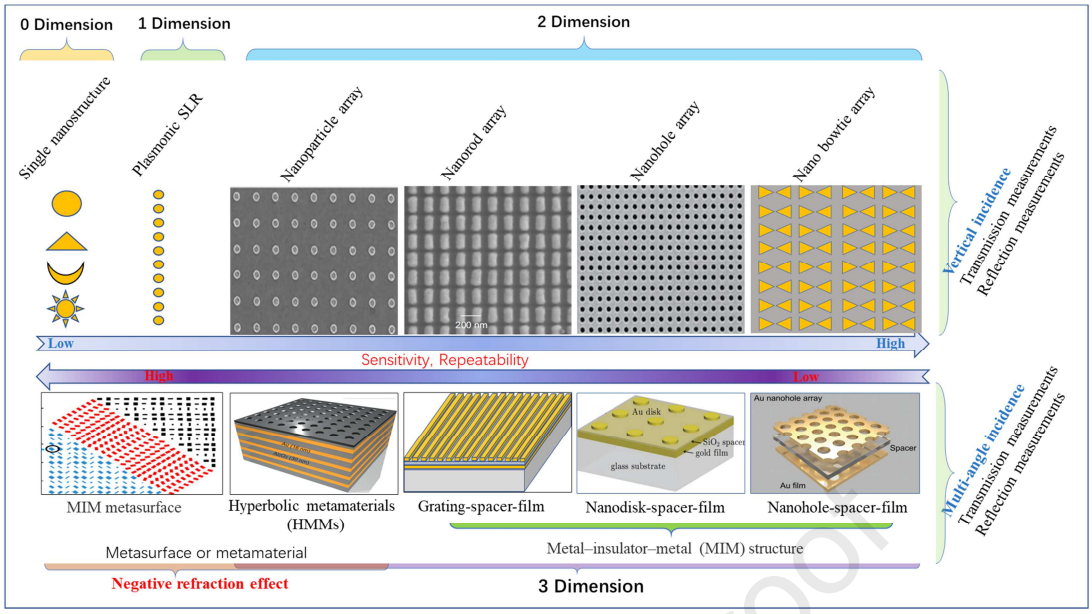

Figure 2. Development trend based on the plasmonic biochemical sensor: from zero-dimensional nanostructure to three-dimensional metal nanostructure, and extending to metamaterial or metasurface.

2.1.2. Array structure

To improve the repeatability, accuracy, feasibility, and uniformity of single nanostructures or disorderly arranged nanostructures in the test, uniform array nanostructures become an alternative solution to enhance the sensitivities of LSPR sensing technology. The electron oscillations are consistent uniform array nanostructures, which is beneficial to the optimization of resonance intensity and resonance peak linewidth (Liu et al., 2020). This uniform array structure and consistent electronic oscillation ensure consistent test results at different test points on the same biochemical sensor chip, which improves the test repeatability and accuracy and promotes this sensing method to a solid step towards clinical application.

Development trends based on the plasmonic biochemical sensor was described in Figure 2. Metal nanostructures range from 0 to 3 dimensions, also extending to metamaterials and metasurfaces. The detailed example would be described as following. The light source is gradually changed from the original normal incident mode to the multi-angle incident. The detection method is gradually changed from the original transmission and reflection test to the multi-angle, multi-spectral reflection, and transmission detection. Multiple measurement data can be obtained simultaneously in multi-angle and multi-spectral testing methods, which can realize self-calibration or self-reference during testing or data processing.

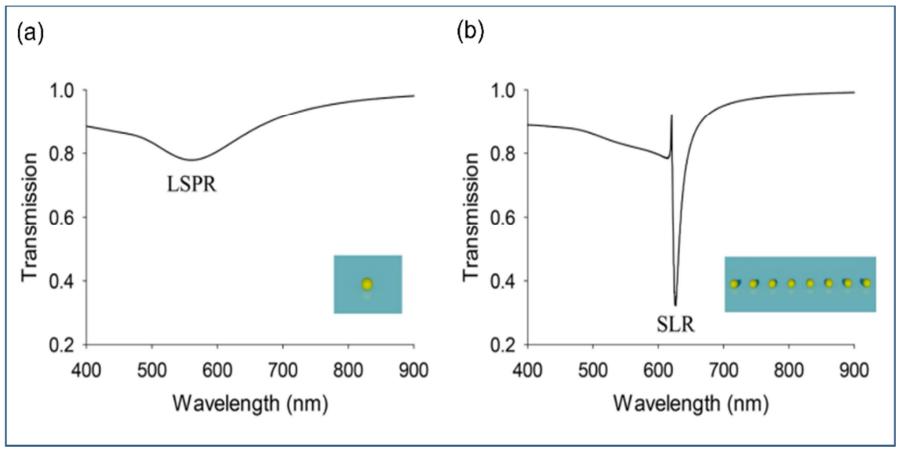

Figure 3. Comparison of LSPR and SLR in transmission spectra. (a) transmission spectra of single-particle; (b) transmission spectra of a periodic 1D chain. Reproduced from (Kravets et al., 2018).

- **Plasmonic surface lattice resonance nanostructure in 1 demention**

The most typical array metal nanostructures are plasmonic surface lattice resonance (SLR) which is to arrange metal nanoparticles in orderly arrays (Kravets et al., 2018). Diffraction waves generated by array scattered light are coupled with local plasmon resonances associated with individual metal nanostructure, resulting in an exciting phenomenon, the drastic narrowing of plasmon resonances, down to 1-2 nm in spectral width, namely, sharp edges of plasmon resonance. The resonance line width is much lower than that of the single nanostructure, which increases the quality factor and the value of the resonance peak. For example, gold nanoparticles with a radius of 80 nm are linear uniform arrangement in one dimension with a regular period of 620 nm. The excitation light incident perpendicularly. And the electric field direction of the incident light is perpendicular to the linear chain. In its transmission spectrum (Figure 3), a very sharp transmission valley at about 620nm wavelength and the transmittance here is as low as about 30%; the transmission spectrum of traditional single gold nanoparticles has a wide trough at about 550 nm, the corresponding transmittance is about 78%. Plasmonic SLR observed in the chain of nanoparticles is much stronger than that of individual nanoparticles and much narrower. FHMW is an almost 10-fold improvement of resonance quality compared with that of single nanoparticle or nanoparticles arranged at random or disorderly. In the case of SLR, near-field coupling leads to the hybridization of the plasmonic modes, which generate antisymmetric modes and provide slightly narrower resonances (FWHM~50 nm). However, these modes cannot easily be excited by incident light. Therefore, A significant improvement in the quality of localized plasmon resonances becomes possible with the involvement of far-field coupling of SLR. By using the right combination of nanoparticle size and shape, coupled with an appropriate array, it is possible to arrange the planar array of light scattered by each nanoparticle with the plasma resonance induction phase in the adjacent incident light, thereby enhancing the resonance of the adjacent particles. Plasmonic SLR (di□ractively coupled local surface plasmon resonance) produces a significant narrowing of the resonance width, as well as associated phenomena such as absorption and significant enhancement of local electric fields near nanostructures. These phenomena are important for a variety of biochemical sensing applications.

- **Uniform array nanostructures**

Several kinds of research on Uniform Array Structure (nanoparticle, nanodisk, nanorod,

nanohole, nanoshell, nanoantennas, nanoribbons, etc.) based on plasmonic biochemical sensing have been carried out, and a series of achievements have been applied to detect the bio-sample, resulting in better repeatability of transmission and reflection spectra, which is helpful to get high performances of the plasmonic biosensor.

Common periodic nanostructures are shown in Figure 4. The period, metal material, and substrate of each array nanostructure would be arranged according to the requirements of the test process, and the preparation would be adjusted to achieve the effect of high sensing.

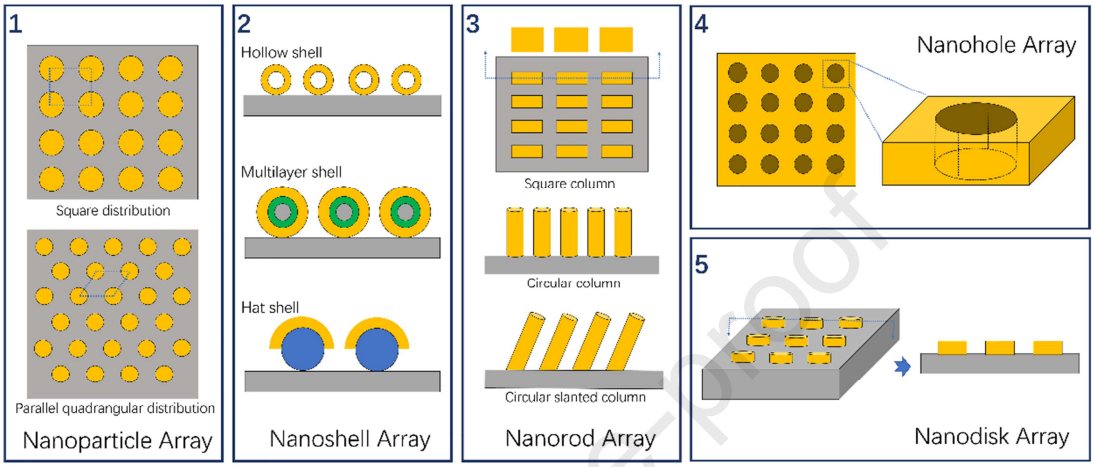

Figure 4. Uniform array nanostructure of nanoparticle (1), nanoshell (2), nanorod (3), nanohole (4), nanodisk (5).

A uniform array nanostructure composed of ordinary spherical nanoparticles is the simplest type of array structure (Figure 4(1)). Compared with a disordered array or a single particle, its sensing performance is more stable and better. This is because the polarization direction of the incident light is consistent with each unit structure of the uniform array, therefore, the resonance modes at each location are coupled very uniformly and strongly. Although the spherical nanoparticle array has the advantages of high sensitivity and narrow linewidth brought by the array structure (Auguié and Barnes, 2008), and also easy fabrication, it is limited by the defect of the shape of the spherical nanoparticle itself. The improvement of sensing performance of uniform nanoparticle array is limited.

As mentioned above, by increasing the contact angle between the particles and the substrate, the spherical nanoparticles would gradually become disc-shaped. For example, in 2019, X. Wang et al developed a kind of disk array to improve sensitivity. The nano-disk array structure consists of a glass substrate, a gold film, a quartz spacer, and a grating from the bottom to the top (Figure 5(1)(a)) (X. Wang et al., 2019). The characteristic was explored with FDTD solution software. Due to the strong coupling effect, the surface plasma is effectively excited, and three resonance modes appear in the reflection spectrum (Figure 5(1)(b)). The resonance intensity of Mode 2 and Mode 3 is extremely large, and the value at the resonance valley almost reaches zero. More importantly, Mode 2 also has a very narrow FWHM, which is very beneficial for RI sensing. Therefore, the RI sensitivity is 853 nm/RIU and FOM_{max} is 126 RIU^{-1}. The results show that the LSPR effect of multi-mode resonance can be detected by sensing from multiple resonance peaks, and the shift of multiple peaks is different, which can be verified by each other. The resonance peaks can also be different according to different test samples. The sensitive resonance peak can be chosen as an important criterion to ensure the validity of each test result.

When the transverse size of nanoparticles is much larger than their height, the nanostructure gradually changes into a nanodisk, and the resonance effect would also change accordingly [56–59]. For example, Khateb et al. proposed an LSPR biosensor based on a gold nanodisk (100 and 200 nm disks) array in 2020 (Khateb et al., 2020b). The results have shown that the thickness of the sensing layer was critical with a significantly larger response for the thinner sample layer. Comparison of differently sized metal nanostructures showed a significantly higher sensitivity for 200 nm diameter compared to 100 nm diameter disk structures resulting from both increases in bulk refractive index sensitivity and the extent to which the local field extends out from the metal surface. These findings confirmed that the developed gold nanodisk-based LSPR sensing chips could facilitate the sensitive detection of bio-samples.

If the nanodisk is elongated longitudinally, the nanodisk gradually evolved into nanorod or nanoantennas. For the sub-wavelength metal nanorods array, the plasmonic Fano resonance or the basic dipole resonance of a single nanorod cannot be simply used to explain its resonance behavior. In 2016, Huang et al. investigated the tightly arranged gold nanorod array (Huang et al., 2016). They proved through simulation that the resonance of the gold nanorod array is caused by the lattice coupling of the multipolar plasma mode. Therefore, the surface electric field strength is greatly improved, which helps to improve the sensitivity in nanoscale from the visible to the mid-infrared. Marae-djouda et al. also discussed the plasma properties of tilted gold nanorod arrays (Marae-Djouda et al., 2018). Since these nanorods are not perpendicular to the substrate, they can detect the coupled plasmon mode in both the vertical and horizontal directions under the illumination of incident light perpendicular to the substrate downward. Coupled with the anisotropy of nanorods, the various plasma modes are coupled with each other, and the gap between adjacent nanorods is extremely sensitive to changes in the refractive index.

The nanoshell array structure has also received a lot of attention from researchers due to its excellent properties. Different shell shapes would have different effects on specific sensing performance, especially the thickness change of the shell layer would directly affect the coupling strength and electric field strength (Zhang et al., 2019). Niu et al. studied a simple gold nanoshell structure (Niu et al., 2020, p. 20). This structure is equivalent to a hollow shell structure formed by removing the middle of spherical nanoparticles (Figure 4(2)). Because both the inner and outer surfaces of the nanoshell structure have the properties of surface plasmon resonance, the surface electric field of the hollow gold nanoshell structure is greatly enhanced. The researchers placed this hollis ow gold nanoshell array structure on the gold film. Thanks to the re-coupling between the array and the gold film, the electric field at the hot spot is further enhanced and the sensitivity is further improved. The results show that the sensitivity of the D-type fiber SPR sensor based on the hollow nanoshell array and the gold film reaches 3064nm/RIU, which is more three times than that of the sensor with only the gold film structure under the same conditions. Paria et al. proposed a silver core-dielectric shell-gold shell (HMCS) multilayer shell structure in the same year (Paria et al., 2019). For better stability and biocompatibility of the gold, the gold shell is set as the outermost layer. In comparison with solid nanoparticles and different shell structures, the researchers also pointed out that adding more shell layers is not conducive to the enhancement of the electric field. From the performance point of view, HMCS is the best choice among the current shell structures. However, due to its relatively complex structure, the time and economic costs would be higher when preparing large areas. There is also a special nanoshell that is different from the above structure. This kind of nanoshell structure is usually called a nanocap, which is a layer

of the metal structure covering the upper part of spherical nanoparticles. W. Cao et al. designed a silver nanoshell array based on microflow injection (Figure 5(2)) (Cao et al., 2019a). They investigated the spectral characteristics and the sensitivity of the silver nanoshell array. Seen from the spectrum in multiple resonance modes, the incident light irradiates the silver nanoshell array to produce LSPR and the surface plasmon wave generates plasma interference when it propagates to the gap between the unit structures of the array. Both of these are sensitive to changes in the refractive index. The results have shown that the sensitivity of the two peaks appearing in the spectrum reached 527.07 nm/RIU and 922.25 nm/RIU, respectively. The quality factor is also very considerable.

Nanohole arrays are usually prepared by perforating a metal film supported on a substrate. Like other array structures, the electric field enhancement of the nanohole array also benefits from the strong coupling of localized and propagating SPR modes. In addition, it also has a special property: the extraordinary optical transmission (EOT) effect (Tokel et al., 2014a). After the incident light is irradiated on the array, removing the part irradiated on the surface, there is a small part of the light through the hole and energy coupling with the SP on the lower surface. The electric field intensity at the hot spot is further increased. On the other hand, the existence of holes also allows environmental media (such as a liquid) to penetrate the structure and the sensitivity of sensing changes in the refractive index is relatively improved (Jia et al., 2020). Jia et al. demonstrated a low-sink method for the preparation of nanohole arrays based on template transport technology (Jia et al., 2013). By repeating the evaporation and transfer of gold, this method makes it easy to prepare a large number of nanohole arrays (Figure 4(3)). Finally, the sensor sensitivity measured in the experiment was 522 nm/RIU. Based on the original work this year, Jia et al. proposed a refractive index sensing platform with a nanohole array on a flexible transparent substrate (Jia et al., 2020). In the experiment, the researchers tested the performance of this sensing platform using different concentrations of sodium chloride solution and deionized water. The results showed that the sensing platform achieved the highest sensitivity of 706nm/RIU and FOM of 52RIU^{-1}. This kind of flexible substrate has good adhesion, disordered surface treatment, more versatile and lower cost, which opens up new application prospects for plasma sensing applications.

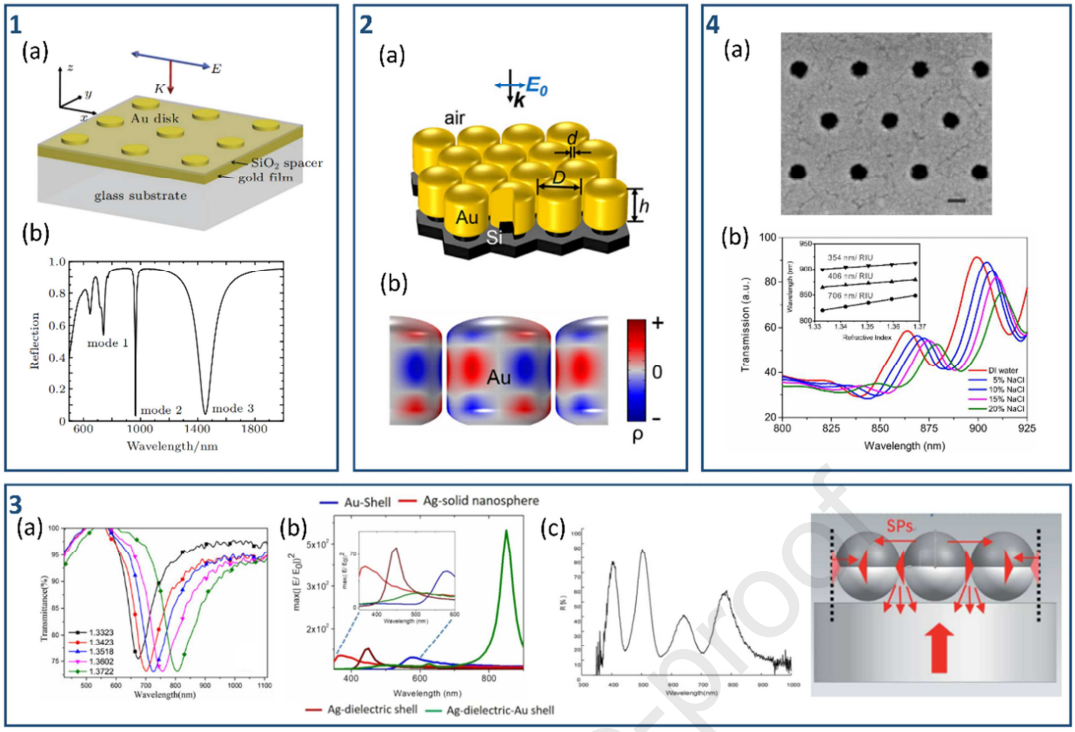

Figure 5. Panel (1) (a) Schematic diagram of the composite structure (the red arrow indicates the direction of propagation and the blue arrow indicates the polarization direction). (b) The reflection spectrum of the composite structure. Reproduced from (X. Wang et al., 2019). **Panel (2)** (a) Schematic diagram of the lattice structure of gold nanorod arrays in the simulation. (b) Corresponding 3D surface charge distributions, indicating the lattice coupling of six-pole plasmon modes. Reproduced from (Huang et al., 2016). **Panel (3)** (a) SEM image of the nanohole array. The scale bar is 200nm. (b) (b) Refractive index sensitivity measurement with water and NaCl solutions of different concentrations. Inset: linear fitting the peak shifts around 830 nm, 860 nm, and 900 nm for respective sensitivity calculation. Reproduced from (Jia et al., 2020). **Panel (4)** (a) Transmission spectrum of the D-type fiber/gold film/Au nanoshell (50/40 AuNS) SPR sensor in different environmental media. Reproduced from (Niu et al., 2020). (b) Comparison of enhancements for the different cases. The inset shows the enhancement at the higher energy peak (zoomed in). Reproduced from (Paria et al., 2019). (c) Sample reflectance spectroscopy and tunable mechanism diagram. Reproduced from (Cao et al., 2019b).

The periodicity of the nanostructure array is a key factor to affect the sensitivity of the LSPR biosensor. The appropriate periodicity relates to the strength of the coupling between the array nanostructures. The smaller period, the closer particle spacing, the stronger electric field at the nanogap could produce a “hot-spot”. As a result, the electric field strength would increase exponentially at a local place (Chung et al., 2019). However, when many particles are very close, the resonance peak may be greatly broadened because of the coupling or overlapping together between the adjacent resonance peaks to form a wide resonant peak, which can guide to reasonably control particle spacing in the design of LSPR biosensing chip.

The light energy scattered by a nanostructured unit cell would be captured by neighboring nanostructures as plasmons rather than attenuated as light traveling in free space, which was used in the coupling between structural units to improve the electric field intensity and hot spot distribution. Therefore, the Q value, wide linewidth characteristic, peak signal ratio, sensitivity, and resonance intensity were greatly improved. However, the array structure requires many

structural units and higher accuracy of nanostructure morphology, which is more complex in the fabrication of nanostructure array LSPR chip. It is comforting that today's micro-nano processing technology continues to develop and advance, which provides a strong possibility to fabricate large area, uniform nanostructure array to improve the sensitivity of LSPR biosensor. Meanwhile, the combination of nanostructure array and microfluidic technology can achieve high-throughput LSPR biosensing. The chip has multiple microfluidic channels and each channel can have multiple nanostructure arrays, which make array-based LSPR biosensor very suitable for multiplexed on-chip detection.

2.1.3. Plasmonic cavity nanostructure

The peak-to-peak signal ratio of LSPR spectra is not large enough, and the resonance peak line width in the characteristic spectrum is too large, which has always restricted its development. To solve this problem, a microcavity structure appeared in the field of vision of researchers. The main reason for the wide spectral linewidth is the existence of radiation damping and energy waste. The microcavity structure can retain the photons entering it to the greatest extent and reduce the scattering loss of excitation light. This allows the photon density to reach a very high level in a small space, suppressing radiation damping, thereby increasing the peak-to-valley ratio of the resonant peak and reducing the line width of the resonant peak; the electric field strength is increased, and the sensor sensitivity is improved. Microcavities are mainly divided into three types, namely Fabry-Perot cavity, photonic crystal microcavity, and whispering gallery mode microcavity. The structures and properties of common plasmonic cavities were presented in Figure 6.

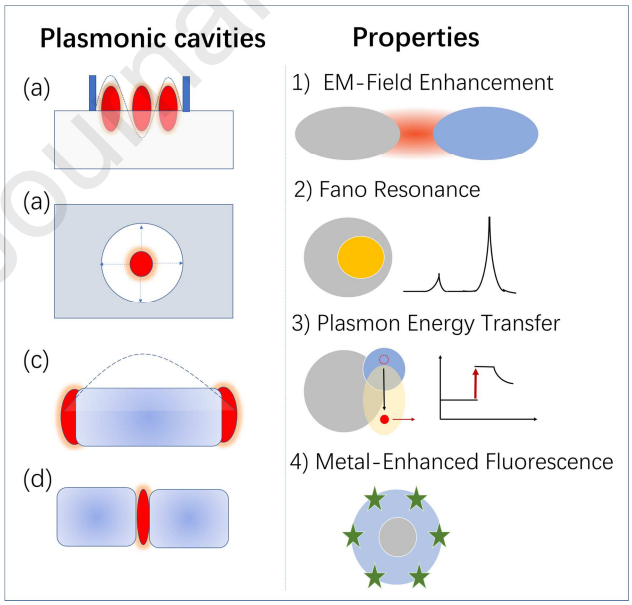

Figure 6. The structures and properties of common plasmonic cavities. (a) Trapped standing wave-type surface plasmon polariton cavities; (b) Localized modes; (c) Dipole antenna and even coupled systems for ultimate EM- field confinement in (d) Gap plasmon systems.

The traditional Fabry-Perot cavity is large and not easy to integrate. Therefore, no further introduction is given here. The photonic crystal microcavity is formed by introducing fine defects into the periodic medium. Its structure is flexible and variable, the manufacturing process is relatively simple and it is also suitable for integration. In 2018, Jung et al. proposed an integrated

label-free detection platform that includes a plasma cavity (Kwon et al., 2018). The incident light is focused by the plasmonic cavity and energy-coupled with the nanoparticle array, resulting in a strong near-field enhancement. Compared with other situations where colloidal gold nanorods or spheres are used to produce LSPR, the plasmonic cavity of the gold and silver cavities is amplified approximately 5-6 times. Hasan et al. designed a cross bow-tie plasma cavity structure that resembles two mutually orthogonal bow knots (Hasan et al., 2015), and the "butterfly wings" part artificially leaves a triangular void. Due to its unique shape, this structure can not only enhance the electric and magnetic fields but also improve the Fano-like dipolar resonance contrast. The results showed large wavelength shifts of 777.5 and 904 nm per refractive index unit (RIU) in dipole resonance and magnetic resonance, respectively.

The whispering gallery mode microcavity, by confining the light in the cavity with total internal reflection and stably spreading. It causes the energy density in the cavity to be extremely large so that high-quality factor can be obtained, while the volume is small and the preparation is relatively simple. Based on the micro-cavity structure of the sensor, the generation of its sensing signal is not from the change of the refractive index of the environment, but the change of the optical path. The molecular binding event increases the length of the optical path in the cavity which in turn causes the resonance wavelength to shift, resulting in a sensing signal that can be recognized by the analytical instrument. Kang et al. studied the gold nano-disk array applied to sensor chips in 2017 (Kang et al., 2017). The nanodisk is located under and in contact with the microcavity structure. The electric field at the contact point is enhanced: the near-field hot spots of ordinary single nanodisk and double nanodisks are increased by about 14 times and 18 times. The energy coupling with the nanodisk can be optimized by controlling the polarization direction of the sensor.

The LSPR sensor based on the microcavity structure has higher sensing performance than the ordinary nanostructured LSPR sensor. This is because the microcavity structure can concentrate the energy of the incident light to the greatest extent and limit this energy to a very small space. This makes the energy density in the space very large and the induced field enhancement is stronger. At the same time, the microcavity structure also improves the energy utilization rate and reduces the radiation loss, so that the LSPR resonance peak has a narrower line width. However, when the microcavity structure is fabricated in a large area, more sophisticated nano-processing technology is required, which puts forward higher requirements for the current nano-processing technology.

2.1.4. Metal–insulator–metal (MIM) nanostructure

The metal-insulator-metal (MIM) structure is a very common structure and is often used as the basis of high-sensitivity sensors. This is because the MIM structure exhibits perfect absorption of light when LSPR occurs (Ghobadi et al., 2017). And its LSPR has nothing to do with the incident angle and light polarization in the infrared region (Ding et al., 2015). When incident light shines on the first layer of metal, the first layer of metal absorbs part of the energy; and the transmitted light passing through the first layer of metal would be absorbed by the second layer of technology. Therefore, the resonance peak-to-valley ratio in the spectrum would be large, and the line width would be relatively narrow. After absorbing the energy of incident light, plasmon resonance occurs in both layers of metal. The two layers of metal are separated by an appropriate distance by the insulating layer in between, so that the resonance coupling between the two can be more

harmonious and stronger. This makes the hot-spots in the structure stronger and the sensor more sensitive.

For example, J. Nan et al. designed a sandwich structure of gold film-interval layer-gold nanohole array, and made an ultrasensitive plasmon scaler platform based on this structure (Figure 7(1)(a)) (Nan et al., 2020). When testing, simply place the object in the middle layer. And the detection platform is clever not only to focus on the refractive index changes but also to flexibly make use of changes in the thickness of the spacer lain by the absorption of biomolecules (Figure 7(1)(b)), which increases the flexibility of the sensing path and makes the sensing more accurate. Thanks to the plasma coupling and the Bloch planar wave surface polaritons., the platform showed ultra-high sensitivity both in the FDTD simulation and in the serum sample detection test. Chang et al. reported a biosensor based on MIM on a flexible substrate in 2018 (Chang et al., 2018). The structure as a whole is a nanodisk array. However, the disk as a unit structure is composed of gold-silica-gold (Figure 7(2)). This sensor can be integrated into a microfluidic chamber to obtain a sensitive microfluidic biosensor. Since the structural parameters of the nanodisk array would greatly affect the sensing performance of the sensor, the researchers optimized the geometric structure of the MIM nanodisk through testing, and thus obtained a sensitivity as high as 1500nm/RIU. Y. Lin et al. proposed two designs of plasmonic metamaterial mid-infrared (MIR) sensors, which are composed of metallic nanograting on SiO_2 layer with a bottom mirror to form metal-insulator-metal (MIM) configurations (Liang et al., 2019). The average S values are approximately constant as 4980 and 4140nm/RIU for MIM-S_2 and MIM-D_2, respectively. Moreover, the maximum FOM can be reached 241.98 for MIM-S_2 and 420.04 for MIM-D_2. Those devices to be used as a compact and multifunctional device integrated into one single chip for wide-spread applications. However, the fabrication is costs high. Lisa P. et al. proposed a multi-layer MIM structure in 2018 (Hackett et al., 2018). The structure is composed of gold-titanium dioxide-gold metal-insulator-metal plasmonic nanocup array (Figure 7(4)(a)). When plasmon resonance occurs, the coupling of the plasmon cavity occurs in the multilayer structure, making its spectral characteristics very sensitive to resonance transmittance and refractive index changes (Figure 7(4)(b)). Through simulation and experiments, this structure has a sensitivity of 800nm/RIU and a detection limit of 10ng/ml.

From the ordinary three-layer MIM structure, multi-layer metal-dielectric layers structure also were presented in the research. A very representative object is the hyperbolic metamaterials (HMMs). Hyperbolic metamaterials have hyperbolic dispersion characteristics because one of their main dielectric constants is opposite to the other two signs (Figure 7(5)(b)) (Sreekanth et al., 2016a). The most important characteristic of this multilayer structure material in sensing is field enhancement: it is extremely sensitive to any change in dielectric constant within the attenuation range of the superstrate. This is because each double-layer structure can excite a propagating SPP wave and the SPP wave would couple with the adjacent double-layer structure. The result of the coupling in turn supports the propagating surface polaron, enabling it to propagate on the interface of each double-layer (Sreekanth et al., 2017). This wave is called volume plasmon.

In 2017, K. Sreekanth et al. proposed a plasma sensor with single-molecule sensitivity based on HMM (Sreekanth et al., 2017). The selected materials for the metal-dielectric layer are gold and aluminum oxide respectively. There are 8 layers in such a double-layer structure. There is an array of nanoholes on the HMM, which acts as a two-dimensional grating to excite the HMM's plasmon resonance (Figure 8(5)(a)). In the experiment, the surface mode of the grating was coupled with

BPP, which made this sensor have extremely high sensitivity from visible light to near-infrared. The structure showed that the sensor achieves maximum spectral and angular sensitivity (around 30000 nm/RIU and 2500°/RIU) at 1300nm and minimum values (13333 nm/RIU and 2333°/RIU) at 530nm. In 2020, Giovanna Palermo and others also took advantage of the excellent performance of HMM for sensing (Palermo et al., 2020). The materials of their double-layer structure are indium tin oxide (ITO) and Ag. They combined HMM with a chiral material with a helical structure (Figure 7(6)(a)) and achieved a maximum sensitivity of 545.5nm/RIU within a refractive index change range of 0.068.

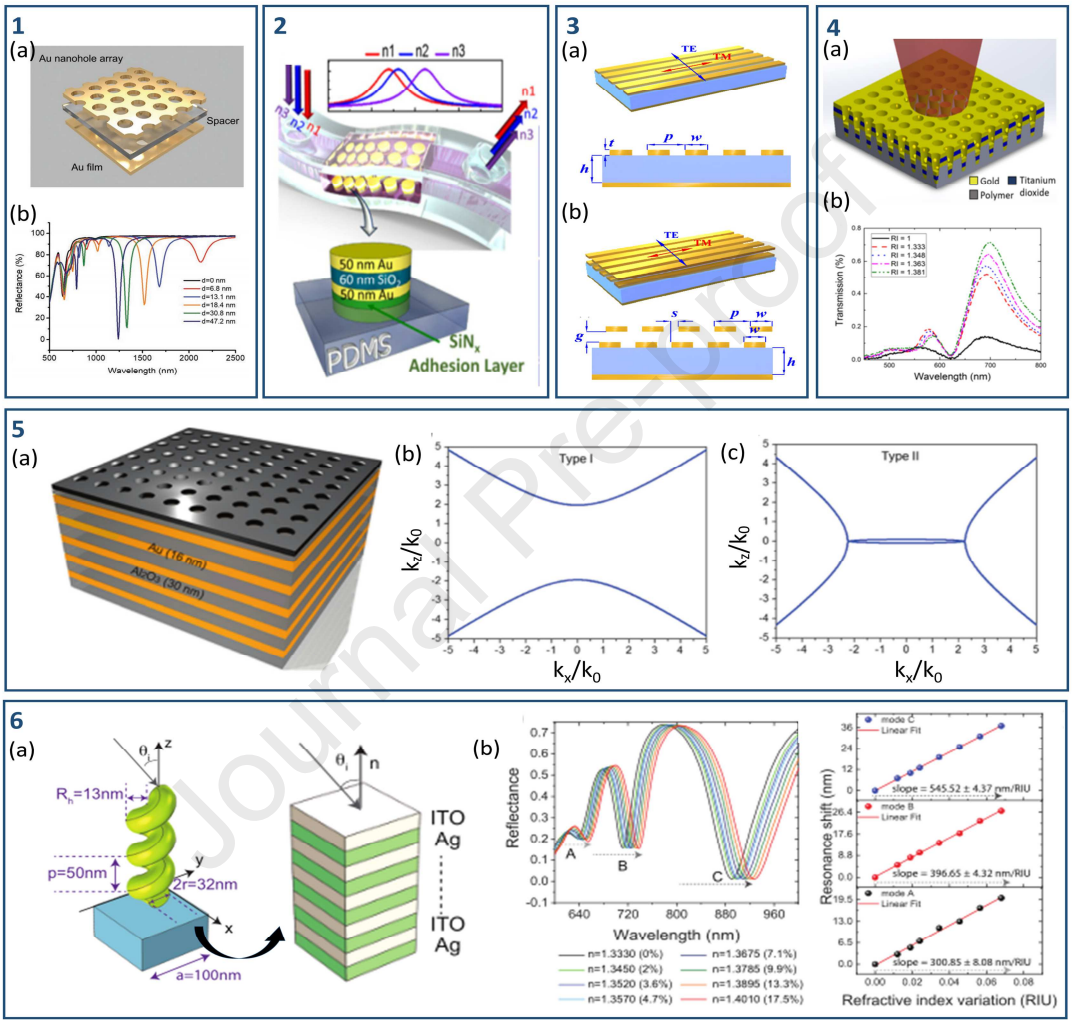

Figure 7. Various MIM structures. **Panel (1)** (a) Schematic of the sandwich structure. (b) Reflection spectra of sandwich structures with different spacer thicknesses. Reproduced from (Nan et al., 2020). **Panel (2)** Schematic diagram of the flexible MIM-disk LSPR refractive index sensor integrated into a PDMS fluidic chamber. Reproduced from (Chang et al., 2018). **Panel (3)** Three-dimensional geometric structure of multi-layer MIM sensor (a) MIM-S and (b) MIM-D. Reproduced from(Liang et al., 2019). **Panel (4)** (a) Schematic and camera image of a wafer-scale MIM nanocup array. (b) Experimental transmission spectra with increasing RI values. Reproduced from(Liang et al., 2019). **Panel (5)** (a) A schematic representation of the fabricated miniaturized diffraction grating coupled HMM sensor. (b) Iso-frequency diagram of two types of HMM (type I HMM and type II HMM). Reproduced from (Sreekanth et al., 2017). **Panel (6)** (a) Schematic diagram of the sensor structure. The picture on the left is the gold spiral structure in the upper part of the sensor structure and the right is the

HMM in the lower part of the sensor. Reproduced from (Palermo et al., 2020).

2.2. Enhance sensitivity by material adjustment

Different materials have different physical and chemical properties due to their microstructure. Therefore, the sensing performance of LSPR sensors would cause huge differences due to different materials. In 2019, Doiron et al. evaluated four types of materials: noble metals, refractory (high temperature stable) metals, transition metal nitrides, and conductive oxides (Doiron et al., 2019a). In the water environment (n = 1.33), they relied on the following two equivalent formulas for calculation: $F_\lambda = \Delta\lambda/FWHM_\lambda \ and \ F_\omega = \Delta\omega/FWHM_{\lambda\omega}$. Where FWHM refers to full-width half-maximum. The result was shown in Figure 8. It has shown the refractive index sensitivity in frequency units (F_ω) and wavelength units (F_λ) with silver outperforming all other materials. As seen from the above calculations, silver as the material of the LSPR sensor is beneficial to the sensitivity of the sensor. However, silver is easy to be oxidized and its instability brings unreliability to LSPR sensing technology. With the advent of new material systems. The high sensitivity of LSPR can be achieved by changing or optimizing sensitive materials. Therefore, we would summary materials to enhance the sensitivity of LSPR sensors from three aspects: metamaterials, two-dimensional materials, and material doping.

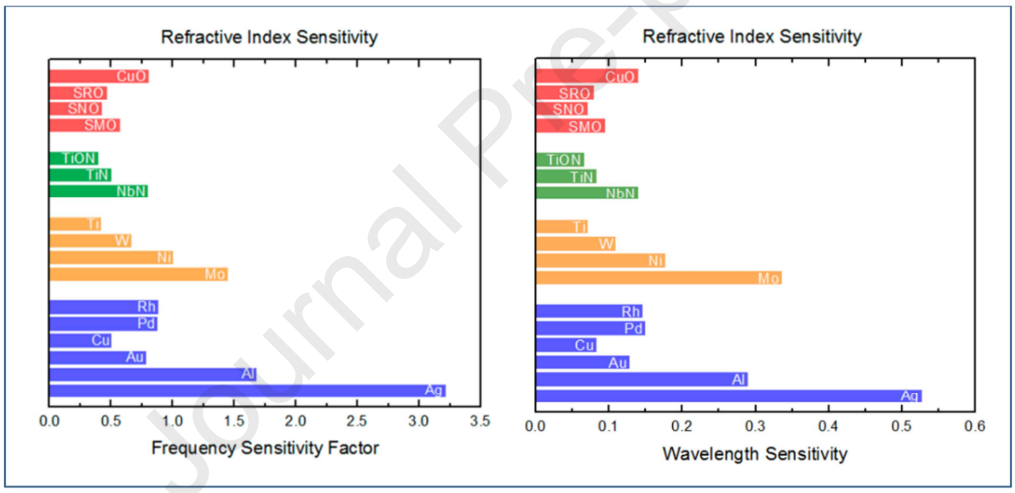

Figure 8. Refractive index sensitivity is calculated in terms of frequency and wavelength. Reproduced from (Doiron et al., 2019b)

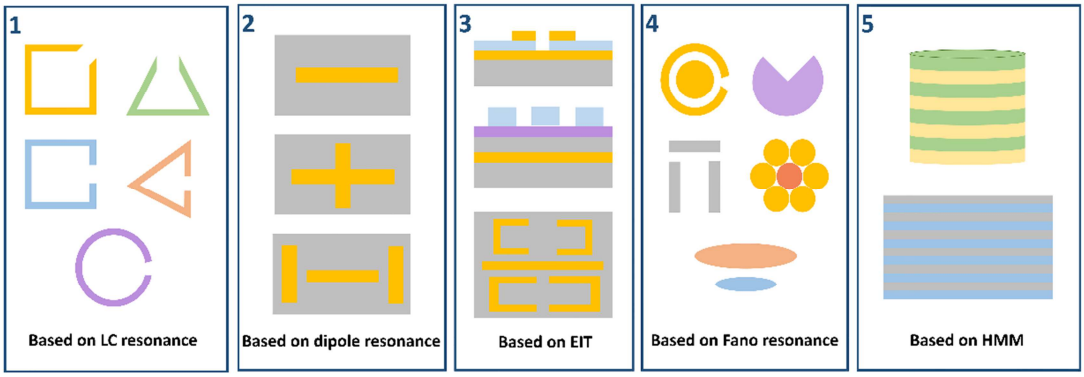

Figure 9. Enhance sensitivity of LSPR based on metamaterials. **Panel (1).** The sensing principle of typical structure based on LC resonance. **Panel (2).** The sensing principle of typical structure based on dipole resonance. **Panel (3).** The sensing principle of typical structure based on the

electromagnetically induced transparency (EIT) effect. **Panel (4).** The sensing principle of typical structure based on Fano resonance. **Panel (5).** The sensing principle of typical structure based on HMM.

2.2.1. Enhance sensitivity of LSPR based on metamaterials

Metamaterials are artificial materials, with optical properties that cannot be achieved using naturally occurring optical materials, can exhibit some amazing phenomena including negative refractive index, strong chiral, and uncertain dielectric constant (Dolling, 2006; Hoffman et al., 2007; Smith, 2004). Metamaterials have strong field localization and enhancement capabilities, which can overcome the limitations of traditional plasmonic sensors and provide a unique platform for biosensing applications (Chen, 2012). Generally, the resonant responses based on metamaterials are mainly divided into four categories: LC resonant mode, dipole resonant mode, and electromagnetic induced transparent (EIT) effect mode, and Fano resonant mode. Therefore, researchers often design and develop many sensors based on metamaterial structure.

- **Based on the LC resonance mode**

Most of the LC resonance modes appear in the open ring structure and the circular ring structure. The fracture of this structure is equivalent to a capacitor (C) and the remaining parts form an equivalent inductance (L), which together form an LC resonance circuit. The metamaterial based on this structure has a simple structure and its characteristic spectrum is highly adjustable, which can be easily achieved by adjusting the structural parameters (Xiao et al., 2017). Coupled with the localization of the strong electric field in the nano-scale gap of the metamaterial, the LSPR sensor based on the metamaterial can show higher sensitivity than ordinary integrated optical sensors. In 2010 Hu Tao et al. Designed a square resonant ring structure with openings on both sides and connected diagonally, called split-ring resonator (SRR) (Tao et al., 2010). The SRR is prepared on the substrate of different thicknesses and materials using micro-nano processing technology. And it is made of gold and 200 nm thick. And in subsequent experiments, the good sensitivity of the sensor based on the silicon nitride substrate was measured., which was significantly improved compared to the sensitivity prepared on the silicon (Si) bulk substrate. And a sensitivity of 2GHz/nm was obtained. But most of the light sources used in the experiments are broadband visible light sources, and broadband light sources are usually non-polarized. This makes the excitation efficiency of the SPP structure based on the LC resonance mode low (Tobing et al., n.d.). Due to the strong polarization dependence, the low efficiency of resonance mode excitation has always affected the full application of the split-ring resonator (SRR). To solve this problem, Xiao et al. proposed a metamaterial composed of four rotating SRRs (Xiao et al., 2017). Due to the rotation of the SRR, this metamaterial introduces asymmetry, so that even and odd resonance modes can be excited at the same time (Figure 10(1)). Three resonance peaks sensitive to changes in the refractive index of the environment appear in the spectrum. Among them, the resonance mode based on the LC model achieved a sensitivity of 1000 nm/RIU.

- **Based on dipole resonance mode**

The most classical resonant unit to excite this mode is a metal bar structure. This structure is like an electric dipole. When it is affected by an external electromagnetic field, it is easy to produce an electric dipole resonance phenomenon. In 2015, Wang et al. designed a dual-band material consisting only of gold strips and a dielectric layer (Figure 10(2)(a)) to overcome the shortcomings of many metamaterials that absorb only in a single band (B.-X. Wang et al., 2015).

They put this material on the gold substrate below. The fundamental frequency resonance excited from a single structure overlaps with the high-frequency resonance generated between the structures. This overlap and the coupling of the plasmon resonance energy of the gold film make the sensor highly sensitive to changes in the refractive index. In the experiment, the fundamental resonance absorption peak was at 1.45THz and the higher-order resonance absorption peak was at 3THz (Figure 10(2)(b)). The FOM and sensitivity corresponding to the two peaks are 1.5, 0.3 THz/RIU, and 34, 2.2THz/RIU respectively, which have great potential for application in practice.

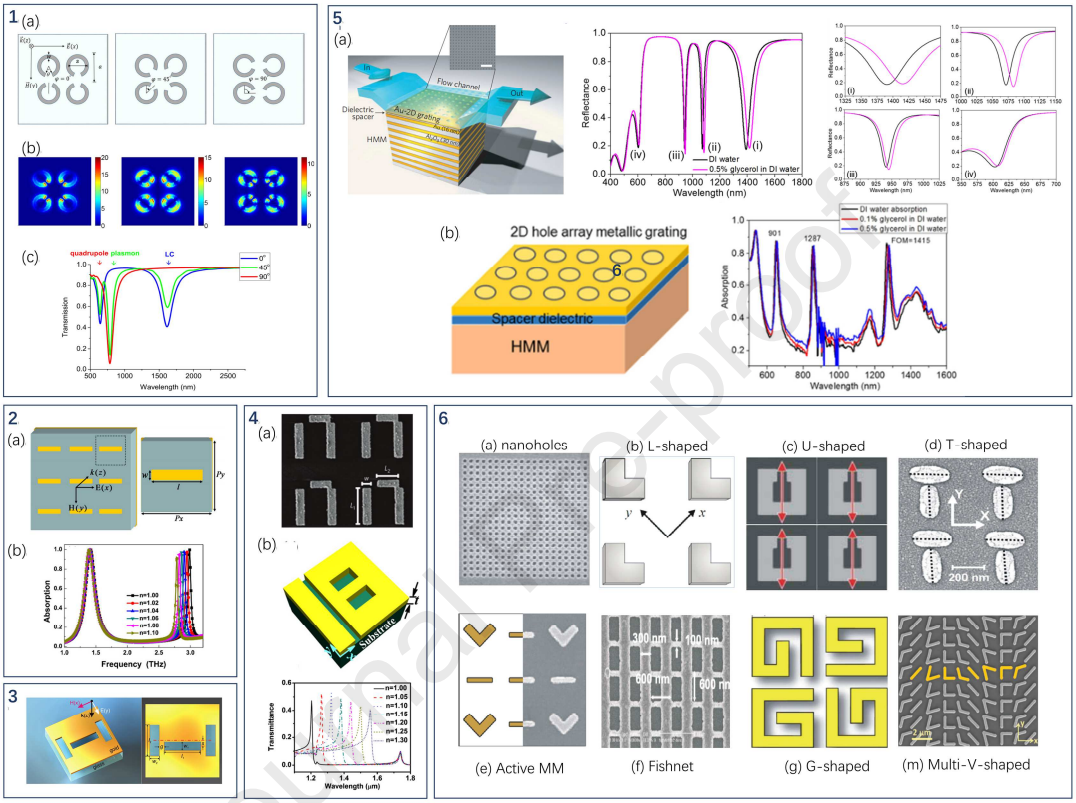

Figure 10. Sensor structures based on different metamaterials. **Panel (1)**. (a) Three quad-supercells of the SRRs with different mutual rotation angles. (b) Electric field enhancement at the angle of 45◦ of an LC mode (N = 1), plasmon mode (N = 2), and quadrupole mode (N = 3) (c) Transmission spectra of metamaterial arrays with different mutual rotation angles. Reproduced from (Xiao et al., 2017). P**anel (2).** (a) The structural schematic of the proposed metamaterial structure. (b) unit cells. Reproduced from (B.-X. Wang et al., 2015). P**anel (3).** Schematic of the planar metamaterial design and the incident light polarization configuration. Reproduced from (Liu et al., 2010). **Panel (4).** (a) Scanning electron microscopy image of a typical fabricated FRAMM. Reproduced from (Wu et al., 2012) (b) Schematic diagram of two metamaterials based on Fano resonant mode and simulated zero-order transmission spectra for different refractive indices of the background in the near infrared band. Reproduced from (Huang et al., 2017). **Panel (5).** (a) Schematic of the HMM-based sensor and Reflectance spectra when distilled water and 0.5% glycerol in distilled water as the superstrate. Reproduced from (Sreekanth et al., 2016a). (b) Schematic of the HMM-based sensor and refractive index sensing of proposed plasmonic absorption sensor using different weight percentages of glycerol in DI water. Reproduced from (Sreekanth et al., 2016b). **Panel (6).** Different structures for metasurfaces. (a)Nanohole; (b) L-shaped; (c)U-shaped; (d)T-shaped; (e)Active MM; (f)Fishnet; (g)G-shaped; (m)Multi-V-shaped. Reproduced from(Glybovski et al., 2016).

- **Based on electromagnetic induced transparency effect**

The electromagnetically induced transparency (EIT) effect is a quantum interference phenomenon. When two beams of light that are close in frequency and are strongly absorbed by a medium at the same time work together on this medium, the medium's absorption of light in a certain frequency band is greatly weakened and becomes transparent. This transparency is often accompanied by great dispersion. However, when this phenomenon occurs, resonance with an extremely narrow linewidth of the absorption spectrum is allowed, which is very meaningful for improving sensor sensitivity and FOM. In 2010, Liu et al. proposed a method to realize EIT using planar complementary metamaterials and applied it to LSPR sensors (Liu et al., 2010). This metamaterial consists of a gold film with an array of cuts on a glass base (Figure 10(3)). Since light excites a bright mode of a dipole and a dark mode of a quadrupole, the induced reflection peaks with narrow spectral characteristics are coupled to produce. Besides, the sensing medium can enter the gap that the performance of the refractive index sensor is further improved. Obvious coupling-induced reflection peaks were observed in the wide resonance spectrum in the experiment, and the sensor sensitivity reached 588nm/RIU. However, EIT-based sensors have certain shortcomings: due to the inherent loss and weak tunability of metals, the quality factor and tunability of EIT in the plasma system would be limited (Lu et al., 2018).

- **Based on Fano resonance mode**

The excitation of Fano resonance is due to the coupling of a discrete localized state to a continuous state (Limonov et al., 2017, p. 2). When Fano resonance occurs, there would be a significant near-field enhancement near the nanostructures, and sharp resonance peaks would appear in the spectrum. When molecular binding events or other events that cause changes in the refractive index of the medium occur, the detection signal would be amplified due to the strong near-field enhancement. This is of great significance for ultra-sensitive detection. C. Wu and others introduced a biosensor technology based on Fano resonance asymmetric metamaterials (FRAMMs) and the detection platform built using this sensing technology break through the limitations of traditional detection (Wu et al., 2012). The metamaterial structure is shown in Figure 10(4): the structure consists of two parallel nano-antennas and one of which has a horizontal coupler. This asymmetric structure makes the excited sub-radiation and super-radiation modes coupled with each other and a strong field enhancement is obtained that the detection signal is also enhanced accordingly. FRAMM arrays provide the possibility for fast biosensor. In 2019, Jung et al. also studied similar structures (Jung et al., 2019). The dark mode excited by the coupler produces a strong spectral response. The dielectric nano pedestal increases the sensing area. The experimental results show that the structure on the nano-substrate obtains a SEIRA signal of more than 7% of the reflection difference, which is 1.7 times the SEIRA signal of the control structure. In 2017 Huang et al. proposed such a metamaterial that its basic unit consists of a narrow slit and two parallel rectangular holes on the same side of the slit (Figure 10(4)(b)) (Huang et al., 2017). Thanks to the interference effect between the coupled SPP with the narrow slit and the coupled SPP with the rectangular hole, the SPP on the metamaterial is enhanced. The resonance peak has an intensity and line width, and they obtained a sensitivity of about 1200 nm / RIU and a FOM value of about 92 in experiments.

- **Based on hyperbolic metamaterials**

Because each two-layer structure can produce SPP and the coupling between adjacent SPPs can also occur, which makes the field enhancement gain brought by HMMs far higher than other

structures. K. Sreekanth et al. proposed a plasmonic biosensor (Figure 10(5)(a)) based on hyperbolic metamaterials (HMMs) to break through the shortcomings of current plasma biosensors (Sreekanth et al., 2016a). The two-dimensional grating with adjustable parameters was used to excite the high-K mode of the hyperbolic metamaterial, and it has a very high sensitivity of 30,000 nm / RIU and a FOM value of 590. In the experiment, reflection spectra were collected in deionized water and deionized water with 0.5% glycerol. The results show that when the refractive index of the external environment changes only slightly from 1.333 to 1.3336, the sensor can still sense it sensitively. It got rid of the huge drawbacks of conventional Kretschmann configuration instruments and provided support for the miniaturization of equipment. In the same year, they also proposed a plasma sensor based on HMM and absorption (Sreekanth et al., 2016b). The structural composition is still grating-dielectric layer-HMM (Figure 10(5)(b)). To increase the sensitivity of the sensor to the environment, the researchers added a microfluidic channel on the top of the structure. Since the SPP generated by the excitation of the HMM and the SPP on the grating surface are coupled with each other, the sensitivities of the three modes of the structure are 23333nm/RIU, 13333nm/RIU and 10000nm/RIU; FOM is 1415, 1287 and 901, respectively.

Table 2: The comparison of different metamaterials sensors.

Author	Structure	Modes of resonance	Sensing performance	Ref.
Xiao et al.	Four rotating SRRs	LC resonant mode	Sensitivity:1000nm/RIU	(Xiao et al., 2017)
Wang et al.	Rectangular strip	Dipole resonant mode	Sensitivity: 2.2THz/RIU; FOM:22.7	(B.-X. Wang et al., 2015)
Liu et al.	Multi-cuts	EIT[#]	Sensitivity: 588nm/RIU	(Liu et al., 2010)
Huang et al.	Narrow slits and holes	Fano resonant mode	Sensitivity: ~1200nm/RIU, FOM: 92	(Huang et al., 2017)
Kandammathe et al.	Gold and alumina films	Multi-resonance	Sensitivity: 30000nm/RIU FOM:590	(Sreekanth et al., 2016a)
Kandammathe et al.	Gold and alumina films or Silver and titanium dioxide films	Multi-resonance	Sensitivity: 23333nm/RIU FOM:1415	(Sreekanth et al., 2016b)

[#]**EIT:** Electromagnetically induced transparency

Table 2 summarizes and compares the characteristics of the above structures. Metamaterial-based sensors usually provide excellent sensing performance, but some issues need to be addressed urgently. For example, the LC resonance-based sensor usually does not have a high Q value, which limits the further improvement of sensitivity. Most metamaterials have complex structures and small sizes, which would be affected by the precision of the processing methods. But the surprise brought to us by metamaterial sensors is still impressive. It is believed that with the further development and deepening of research, the potential of metamaterial-based refractive index sensors in the fields of high sensitivity and high accuracy sensing and detection would be further explored.

- **Based on plasmonic metasurface**

The plasmonic metasurface is a two-dimensional metamaterial system based on sub-wavelength nano-elements with specifically designed geometry, size, and orientation assembled into arrays to locally control electromagnetic fields(n.d.). Common metasurface structures are shown in Figure 10 Panel 6 (not limited to Figure 10 Panel 6) (Glybovski et al., 2016), which need uniform periodic nanostructures, fine features, and large-area patterns via a low-cost and reproducible fabrication process. The unique properties of plasmonic metasurface in the changing dielectric environment would extend the application in biosensing with high sensitivity compared with traditional LSPR biosensor chip(Zhu et al., 2020). Many efforts have been carried out to improve the performance of LSPR biosensors by using various nanostructured metasurfaces (Cai et al., 2019; Glybovski et al., 2016; Narasimhan et al., 2020; Siddique et al., 2019; Tittl et al., 2019; Z. Zhang et al., 2020; Zhu et al., 2020). Considerable progress has been made in label-free biomolecular sensing based on plasmonic metasurface, which benefits from the nanoscale near-field enhancement with high sensitivity and non-destructive operation for high-throughput real-time detection. For example, in 2020, J. Zhu, et al. presented the low-cost flexible bio-functionalized plasmonic metasurfaces with periodic gold nanobumps on a flexible lightweight polycarbonate substrate for highly sensitive label-free detection of tumor marker in human serum samples. The sensitivity reaches 454.4 nm/RIU. The results illustrated that the flexible plasmonic metasurfaces demonstrate promising potential for future portable medical devices/systems in point-of-care diagnosis and mobile healthcare. In 2019, et al. used a plasmonic metasurface composed of aluminum nanocavity antennas to overcome the disadvantage of aluminum-based nanoantennas with poor plasmon performance in the visible light range (Siddique et al., 2019). When resonance occurs, there were hybrid multipolar lossless plasmonic modes in the cavity, which greatly enhances the local field. It made these nano-antennas highly efficient in the visible light range, which greatly increased the sensitivity. The results showed that in the visible wavelength range, the plasmonic metasurface structure can increase the detection ability of molecules by more than 1000 times compared with the glass control sample. Usually, the structures of plasmonic metasurface have a distinguishable spectrum and an LSPR mode that can be addressed individually and simultaneously, showing the potential of 3D sensing, which imply a direction for jumping out of the limitation of only being able to detect processes occurring in the plane of the array.

2.2.2. Enhance sensitivity of LSPR based on 2D materials & transition metal dichalcogenides (TMDs)

Despite uniform array nanostructure with “hot spot” could be used as an effective means of increasing the reaction surface and generating a very confined localized surface plasmon mode, and therefore, enhancing a polarized field-nanoparticle interaction, new method to enhance sensitivity is still on the way. For example, because two-dimensional (2D) material has the characteristics of a high surface-area-to-mass ratio and some special properties that are different from conventional materials, to improve the sensitivity, in addition to the methods mentioned above, two-dimensional (2D) nano-layers also has been applied to enhance sensitivity (Koppens et al., 2011). The large surface area of two-dimensional material allows more sensing molecules to be fixed on it, which illustrated that it is a very high potential biosensor platform (Kaul, 2014; Li et al., 2014; Tang and Zhou, 2013; Zhang and Xie, 2013). The most typical LSPR sensor chip structure combining two-dimensional materials and nanostructures is shown in Figure 11. One

structure is to prepare various nanostructures on the two-dimensional material surface (Figure 11(a)). Another structure is in the nanostructure table covered with a layer of two-dimensional material (Figure 11(b)).

Graphene is the best-researched as well as the oldest 2D nanomaterial and has the same properties as precious metals in the infrared and terahertz bands (Gan et al., 2012; Wang et al., 2008), which can excite the surface plasmon to support the propagation of SPP waves. What's more, graphene has a stronger ability to bind plasmons to the surface than that of metals. And it can regulate the surface plasmons excited on the surface by regulating the applied electric and magnetic fields (Lu et al., 2013; Woessner et al., 2015a). Meanwhile, graphene was considered as a very promising new kind of material with possible applications in bio-plasmonics (Woessner et al., 2015b). Therefore, many scholars have carried out researches on sensing properties based on the combination of graphene and metal (gold or silver) nanostructures (Cen et al., 2018a; El barghouti et al., 2018a; Tsai et al., 2011; Woessner et al., 2015b; Zhao et al., 2013a), and the main structure is shown in Figure 11. The sensor sensitivity is shown in Table 3. Some scholars have even introduced micro-nano fluid technology into such sensors to reduce sample consumption and increase their sensitivity to miniaturize chips. For example, Peng et al combined graphene films and aluminum substrates to propose a tunable absorbent material that can be used as a refractive index sensor (Zhou and Zheng, 2018). Graphene was used to enhance the intensity of evanescent waves, thus strengthening the energy coupling and improving the sensitivity. In the same year, Cen et al. designed a plasma refractive index sensor for graphene nanobelt arrays (Cen et al., 2018b). The sensitivity can be improved by adjusting the length of the banded structure. The research results presented in numerous literatures indicate that the variation of metal type, structure and layer number of two-dimensional materials, or relative position of both, are frequently discussed factors in the study of LSPR sensing characteristics.

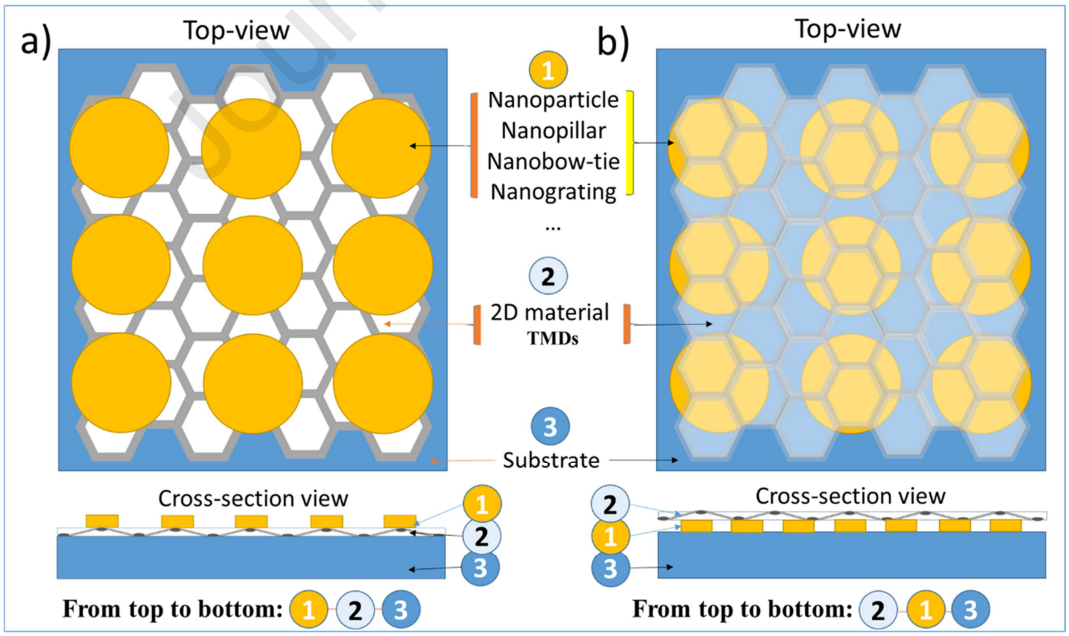

Figure 11. Schematic diagram of the LSPR sensor based on two-dimensional materials. (a) Metal nanostructure on the surface of 2D material; (b) 2D material covers the metal nanostructure.

Broadly speaking, transition metal dichalcogenides (TMDs) also is two-dimensional material,

which has good rigidity and abrasion resistance, and molybdenum disulfide has received wide attention as representatives. Therefore, TMDs were used to enhance the sensitivity of LSPR. Metal nanostructures combine with TMDS to form LSPR sensors, and MoS_2 is the most typical TMDS material due to the good bonding between S (sulfide atom) and metal atoms (gold or silver). For example, Liu et al. used an angle-resolved reflectivity method to illustrate that there is a strong coupling effect in the single-layer MoS_2 integrated silver nano-disk array: strong exciton-plasmon coupling (Liu et al., 2016). This strong coupling significantly improves the light absorption properties of the nanoparticles. Mohamed El Barghouti and others developed a new configuration method of LSPR ultra-sensitive biosensor based on MoS_2 film: separation of gold nanoparticles and detected dielectric media using MoS_2 film as the spacer (Barghouti et al., 2018). This configuration method results in the strong coupling between the gold nanoparticles and the thin film, and the resonance peak of the gold nanoparticles appears a significant redshift. In the experiment, the corresponding plasmon resonance wavelength increases by 333.7 nm when the thickness of the MoS_2 film is 3.90 nm. Based on the good characteristics of MoS2, their team quantitatively studied the sensitivity of the coating thickness of MoS_2/AgNPs/glass on MoS_2 in their subsequent work (El barghouti et al., 2019). It is found that when the thickness of the MoS_2 coating reaches 13.2nm, the sensitivity can reach 121nm/RIU due to the strong plasma coupling between the silver lattice and the MoS_2 layer. In 2015, Butun et al. found that the nanodisk array on the MoS_2 film would be coupled with the MoS_2 film due to plasmon resonance, which greatly enhanced the electric field (Butun et al., 2015). This is a good reference for improving sensor sensitivity.

Table 3: The comparison of sensors based on graphene.

Author	The way to use graphene	Sensitivity	Ref.
Mohamed et al	AgNPs deposited on a glass substrate and coated with a graphene	106 nm/RIU	(El barghouti et al., 2018b)
Zhao et al.	Graphene was located on the substrate in direct contact with biomolecules in the sensing medium.	1697nm/RIU	(Zhao et al., 2013b)
Wei et al.	Graphene sheet covered the top of the nanochannel.	1920nm/RIU	(Wei et al., 2014)
Peng et al.	Graphene was coated on alumina spacer	223nm/RIU	(Zhou and Zheng, 2018)
Cen et al.	Nanoring-strip graphene arrays were placed on sensing media	2970nm/RIU	(Cen et al., 2018b)

2.3. Enhance sensitivity by interface modification

The surface modification methods of gold nanostructures are also different according to the different test targets. The active area of the LSPR biosensor enables the recognition element to be stable and allows them to interact with the target analytes. There are several surface modification techniques such as physical adsorption, chemical adsorption, covalent binding, and a□nity-based interactions to immobilize the recognition element, which is relative to the sensitivity, specificity,

and limit of detection. Besides these common methods, recent advances in surface functionalization and antifouling agents to minimize nonspecific binding are also reviewed in the following subsections. Due to space limitation, this paper is limited to important methods to improve the sensitivity of LSPR sensor. Table 4 summarizes the **interface modification** methods to enhance the sensitivity briefly. To increase sensitivity, surface modification methods would be briefly introduced one by one.

2.3.1. Modified on metal nanostructure to enhance LSPR sensing signal

To effectively improve the sensitivity, gold nanoparticles (AuNPs) are often used as a means of signal amplification because it further enhances the plasmon resonance coupling and enhances the detection limit (Cao et al., 2011; Ertürk et al., 2016; Hong and Hall, 2012; Huang et al., 2018; Wang et al., 2009; Yuan et al., 2007). R.P. Van Duyne et al first proposed using nanoparticles to amplify signals (Hall et al., 2011). In 2011, he and co-authors developed a method to amplify the wavelength shift observed from LSPR bioassays by using gold nanoparticle-labeled antibodies, which involves detecting surface-bound analytes using gold nanoparticle conjugated antibodies, provides a way to enhance LSPR shifts for more sensitive detection of low-concentration analytes. The results have shown that there were 400% amplification of the shift upon antibody binding to the analyte. The amplitude of the signal increased by two times, and the detection limit increased by three times (Figure 12(1)). Ko et al. introduced gold nanoclusters (AuNCs) composed of AuNPs aggregates as signal amplifiers in the experiment (Figure 12(2))(Ko et al., 2019a). The presence of AuNCs enhances the coupling between AuNPs at the LSPR interface and leads to an increase in the number of specific target molecules bound to the bioassays, significantly improving the intensity and displacement of the LSPR resonance spectra.

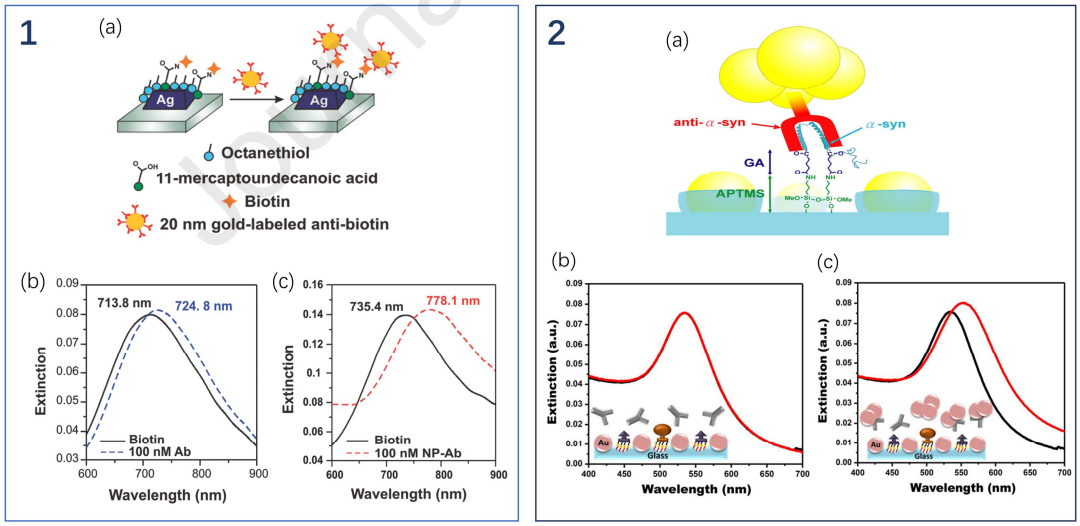

Figure 12. Experiment schematic and LSPR spectra of LSPR chip by using nanoparticles to amplify signals. **Panel (1)**. (A) Biotin is covalently linked to the nanoparticle surface using EDC coupling agent, and anti-biotin labeled gold nanoparticles are subsequently exposed to the surface. LSPR spectra are collected before and after each step. (B) LSPR spectra before (solid black) and after (dashed blue) binding of native anti-biotin, showing a $\Delta\lambda_{max}$ of 11 nm. (C) LSPR spectra before (solid black) and after (dashed red) binding of anti-biotin labeled nanoparticles, showing a $\Delta\lambda_{max}$ of 42.7 nm. Reproduced from (Hall et al., 2011). **Panel (2)**. (A) Schematic representation of plasmonic coupling in terms of gold nanoparticle-based clusters on AuNP-based LSPR biochip. change for the immunoassay without

(B) and with (C) conjugation of AuNCs aggregated from AuNPs 10 nm in size. Reproduced from (Ko et al., 2019a).

The observed enhancement in LSPR shift is produced by a combination of two mechanisms: (1) An overall increase in refractive index change upon antibody binding due to the presence of a gold nanoparticle, and (2) plasmonic coupling between the gold, nanoparticle label, and the nanostructure substrate. The degree of plasmonic coupling depends on several factors including nanoparticle size, Interparticle short, and nanoparticle orientation. Many researchers hope that the observed LSPR displacement can be further enhanced by increasing the size of the nanoparticle marker or by controlling the orientation of the antibody to bring the marker closer to the nanoparticle substrate. Thus, the use of gold nanoparticle tags provides a way to meet the growing sensitivity needs of diagnostic equipment. When applied to related biological systems and biomarkers, this technique can significantly improve the detection limit of disease diagnosis.

The principle of modifying metal nanostructure to improve the sensitivity of the sensor is very simple: the coupling between the modified metal material and the precious metal nanoparticles used for sensing strengthens the electric field strength and enhances the plasma resonance, thereby amplifying the sensing signal. It is a common and effective method for improving the sensitivity of sensors and reducing the detection limit.

Table 4: Methods to improve the sensitivity of LSPR sensor by interface modification.

Interface modification	Method	Principle of increased sensitivity
Modified metal nanostructure	Gold nanoparticle conjugated antibodies	Enhanced coupling and increased electric field strength.
Modified on different biological samples to link the target sample	Adding protein G.	Increase the number of detection antibodies on the sensing surface.
	ELISA	Enzymatic reaction generates high refractive index precipitation, which greatly changes the refractive index of the environment near the surface of the LSPR biosensor.
	Adding secondary antibody	Increase molecular binding events, amplify signals, and improve selectivity.
	Aptamer	Small size that the location of molecular binding events is closer to the sensing surface.
	Thiolated DNA molecule	Increase the number of detection molecules.

2.3.2. Modified different biological samples to link the target sample to enhance LSPR sensing signal

The chemical conjugation of the active surface of LSPR biosensor to increase its selectivity or specificity determines the effective and extensive application of LSPR biosensors in biological analyses since the extraction of the target analyte from the biological solution by means of consolidated protocols su□ers great limitations at low analyte concentrations(Cohen and Walt, 2019; Culver et al., 2018; Ha et al., 2019; Hall et al., 2011; Kalia and Raines, 2010; Ko et al., 2019b; Masson, 2017; Oliverio et al., 2017b; Reimhult and Höök, 2015; Saha et al., 2012; Tokel et al., 2014b; Vashist et al., 2014). The typical working mechanism of an LSPR biosensor chip

and the pivotal role of the surface functionalization are shown in Figure 13.

Usually, the LSPR sensing signal is proportional to the metal surface coverage, which is dependent on the concentration in the added sample after equilibrium has been established and therefore a uniform coverage is preferred. Hence, the functionalization of nanostructures with molecular complexes able to interact with the target analyte concentration drastically improves the sensitivity, defined as the variation of the biosensor signal as a function of the variation of the analyte and selectivity, identified as a di□erence in the response of the device to di□erent analytes. These new platforms may revolutionize the field of biosensing if e□ectively combined with the proper surface chemistry able to capture the analytes directly from raw biological fluids.

Therefore, in terms of inter-surface modification, the specificity of analyte recognition, the orientation of the immobilized biomolecules acting as the analyte receptor, the selectivity of surface coverage, the efficiency of target sample bonding, the metal active area, and the inert area should be effectively considered or appropriate treated, which is related to the performance of the LSPR sensor (sensitivity, repeatability, reliability). Immobilizing biomolecules in the correct direction on the surface of the sensing metal can effectively improve the recognition efficiency between molecules and reduce the specific recognition of other non-target molecules. The specificity between the recognition element and the target detection object means strong intermolecular affinity, which implies that the target analyte can be detected more sensitively under the same conditions. It also ensures the accuracy of sensing. To isolate the non-sensing part of the sensor to reduce the interference of the non-sensing part to the sensing part directly or indirectly affect the detection sensitivity of the LSPR biosensor.

In the process of fixing biomolecules on the sensing metal surface, in addition to the small number of fixed biomolecules (such as antibodies), their poor orientation would also directly affect the detection sensitivity of the sensor. First, for the orientation of the modified molecule, the most widely used and effective strategy is to use an intermediate connector to connect the sensing surface and the biometric original. According to the different principles, this strategy is divided into two types: the coupling method based on covalent bonding and the coupling method based on affinity. The former usually use bifunctional thiol as a linker to create molecular self-assembly (SAM) on the metal surface and then connects the linker to the complementary functional groups on the biomolecule through organic chemical reactions.

Affinity-based surface functionalization technology is also often used to immobilize biomolecules due to its advantages of not affecting biological structure and function. In the process of fixing biomolecules on the sensing metal surface, in addition to the small number of fixed biomolecules (such as antibodies), their poor orientation would also directly affect the detection sensitivity of the sensor. Adding protein G is an effective way to solve these problems. Protein G is an immunoglobulin (IgG)-binding bacterial cell wall protein isolated from group G streptococci. In 2012, Wang et al. found in experiments that the addition of the Protein G allowed more antibodies to be immobilized on the surface; and in terms of antibody binding, Protein G-based surface chemistry significantly improved the capture efficiency (Wang et al., 2012). Therefore, the results illustrated that the sensitivity and detection limit of the sensor can be improved in this method.

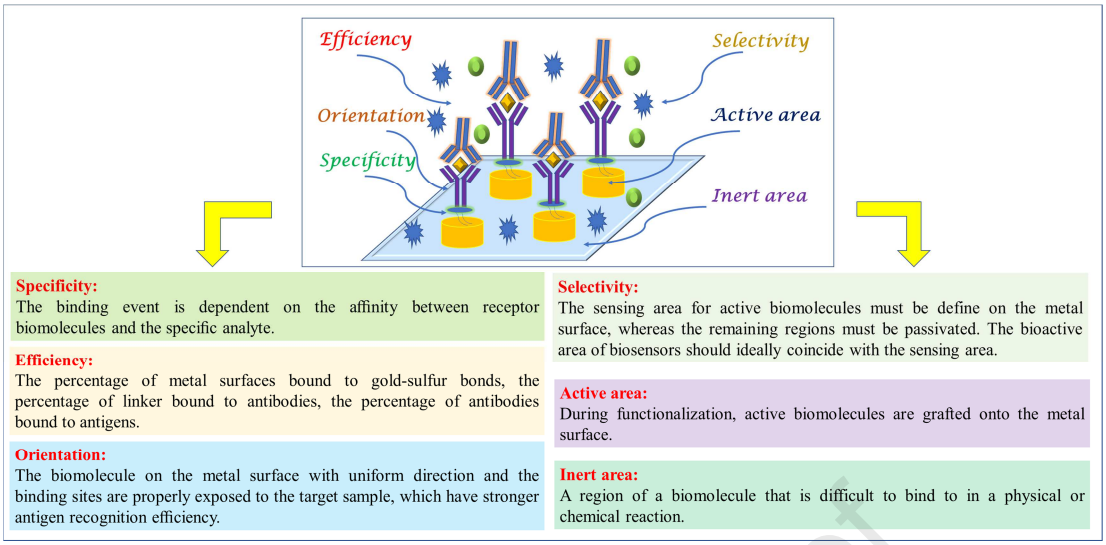

Figure 13. Pictorial description of six aspects of LSPR biosensor functionalization**.**

Using enzymatic reactions to amplify the LSPR resonance peak shift can effectively improve the sensor sensitivity. Enzyme-Linked Immunosorbent Assay (ELISA) is an important method for studying protein antibodies. Si Chen et al., based on the progress of enzyme protein signal enhancement in biosensors (Lee et al., 2011; Pita et al., 2008), combining local plasmon resonance and ELISA techniques, successfully demonstrated that the peak shift for LSPR resonance peaks caused by one or more horseradish enzyme activities can be measured increasing the sensing sensitivity close to the single-molecule limit (shown in Figure 14) (Chen et al., 2011a). The experiments first biotinylated gold nanoparticles shaped like a round table, using biotin can combine the characteristics of anti-pectin- horseradish peroxidase (HRP) enzyme molecules conjugate, gold nanoparticles, and conjugates can be linked together, and then through this conjugate can catalyze the particle surface reaction to produce high refractive index precipitation, resulting in an increase in LSPR resonance peak shift, thus improving the sensitivity of the sensor. Many studies have shown that the LSPR effect of gold nanoparticles combined with the modification of ELISA for colorimetric display can more effectively and intuitively apply the sensing technology of LSPR effect (Chen et al., 2015, 2011b; Gao et al., 2020; Kaewwonglom et al., 2019), and even combined with the lateral flow technology can make the LSPR-ELISA composite detection method based on gold nanoparticle materials to the clinical application (Gao et al., 2020).

In immunological detection, the presence of secondary antibodies can effectively improve the antigen-binding efficiency, thereby reducing the detection limit (Lee et al., 2013); the specific binding events between the target molecules are increased at the same time and the shift of the resonance peak is amplified, thereby improving the sensitivity of the LSPR sensor.

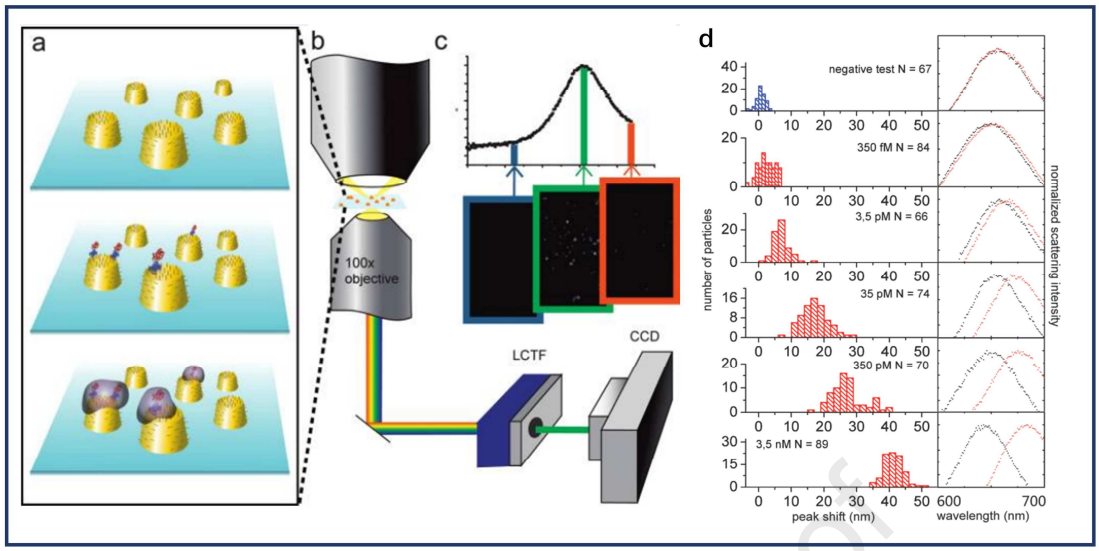

Figure 14. Schematic of the experimental process for typical LSPR chip combined with ELISA. (a) Gold nanostructure surface modification process. (b)-(c) Detection and recording of signals. (d) The test results under different steps of the experimental process. Reproduced from (Chen et al., 2011a).

The traditional antigen-antibody detection method modification process is described as following: firstly, gold or other metal nanostructures modify thiol; secondly, using EDC to activate the carboxyl group of thiol and connect with the antibody. Finally, the specific binding of antigen-antibody is used to detect the target molecule. Although this modification process is not complicated, the whole process takes a long time, and the chemical reaction conditions of each step are strict. Therefore, the reaction time needs to be reduced and the modification process simplified. Surface modification aptamers for gold nanostructures would be the simplest method. Therefore, aptamers are also frequently used as a recognition element. Aptamers are capable of specifically binding an analyte with an a□nity comparable to antibodies. To fix the aptamer on the surface of gold nanostructure to obtain the detection target molecule, it only needs to connect the gold nanostructure and the aptamer through thiol, without activation. Moreover, the LSPR biosensor modified with aptamers is more sensitive than the traditional sensor modified with antibodies. The LSPR biosensor uses the principle that the change of the refractive index of the surrounding environment can cause the corresponding spectrum to shift. However, when LSPR occurs, the electric field near the gold nanostructure decays exponentially in the vertical direction. Therefore, when the position where the change of the environmental refractive index occurs is far away from the sensing part, the sensitivity of the LSPR sensor would be greatly reduced (Doiron et al., 2019a). For example, Seongjae et al. developed an LSPR biosensor modified with an aptamer. Schematic illustration of the steps involved in the sampling of salivary cortisol and detection of salivary cortisol using the LSPR aptamer-sensor shown in Figure 15(a). The spectral shift caused by the target molecule (the spectral peak shift of the sensor modified with aptamer was greater than that of the sensor modified with antibody (Figure 15(b) and (c)). Meanwhile, the authors measured the physical sizes of the nanoparticles after modification (Figure 15(d) and (e)). The results illustrated that the average height of the antibody and aptamer in the experiment and found that the average height of the antibody to aptamer was about six times that of the aptamer. Therefore, after binding the target molecule, the binding site of the modified antibody would be farther from the sensing part than the binding site of the modified aptamer. The relative sensing

volume of the modified antibody is smaller than that of the modified aptamer. This leads to better sensitivity of the modified aptamer LSPR sensor. Moreover, due to the large size of the antibody, the number of modifications on the gold nanostructure is also less than that of the aptamer. This is also why the aptamer-modified LSPR sensor is more sensitive than the modified antibody.

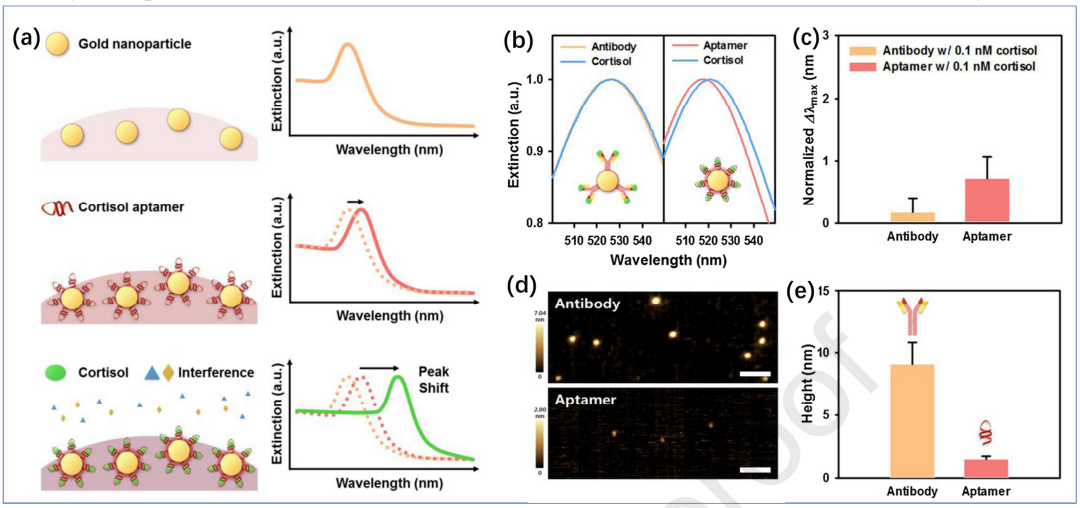

Figure 15. Schematic illustration of the experimental steps and results. (a) Schematic illustration of the steps involved in the sampling of salivary cortisol and the detection of salivary cortisol using the LSPR aptamer-sensor. (b) Extinction spectra showing the extinction peak shift of AuNPs immobilized via the aptamer or antibodies, before and after cortisol treatment. (c) Normalized extinction peak shift ($\Delta\lambda_{max}$) of AuNPs immobilized via the aptamer and antibodies following cortisol treatment. (d)AFM images of antibodies and aptamer (Scale bars: 250 nm). (e) Height analysis of antibodies and aptamer. Reproduced from (Jo et al., 2020).

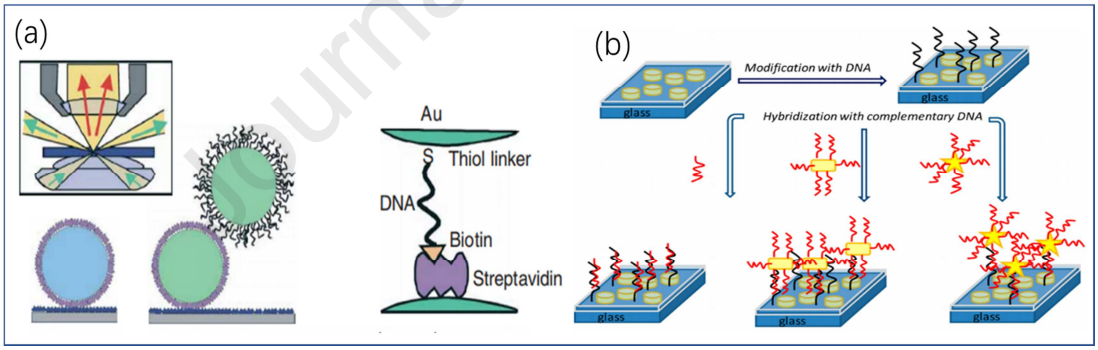

Figure 16. (a) Schematic illustration of directional assembly and surface modification of nanoparticles. Inset: the principle of transmission darkfield microscopy. Reproduced from (Sönnichsen et al., 2005). (b) Schematic illustration of the hybridization process of the DNA-functionalized LSPR chip with unlabeled complementary DNA and gold-nanostructures labeled DNA molecules. Reproduced from (Spadavecchia et al., 2013).

The rational use of aptamer reaction conditions seems to be a suitable solution. The binding of the aptamer to the target molecule on the sensor is reversible. When the sensor is used, the reaction condition becomes the positive direction condition that is favorable for the binding reaction between the aptamer and the target molecule; when the sensor is recovered, the control reaction condition becomes the negative direction condition that is favorable for the dissociation reaction (Cathcart and Chen, 2020). Therefore, a reasonable adjustment of the detection environment is also the key to improving the strength of the sensing signal.

The modification of DNA molecules on gold nanostructures is also a simple and practical method. For example, Carsten et al. performed real-time tracking of the directional assembly of gold and silver nanoparticle dimers and investigated the kinetics of individual DNA hybridization events in the process (Sönnichsen et al., 2005). They bonded single-stranded DNA (ssDNA) on the second particle of the dimer (Figure 16 (a)), found that the spectral offset did occur apparently after DNA hybridization, and verified that the reason for the spectral offset was DNA hybridization by comparing the spectral positions before and after the addition of complementary and non-complementary DNA. Jolanda et al. used thiolated DNA molecules as an amplifier for DNA hybridization detection in 2013, combined with gold nanostructures, successfully improved their detection sensitivity several times higher than that of unlabeled DNA systems (Spadavecchia et al., 2013). Figure16 (b) is a schematic diagram of the hybridization process.

Table 5: Comparison of different modification methods.

Author	Modifier	Performances	Ref.
Ko et al.	AuNCs	Detection limit: 3.8 ng/mL	(Ko et al., 2019a)
Si Chen et al.	Streptavidin-HRP conjugate	Bulk sensitivity: 100nm/RIU	(Chen et al., 2011a)
Jo et ai.	aptamer	LOD: 0.1 nM	(Jo et al., 2020)
Loyez et al.	aptamer	LOD: 10 cells / mL.	(Loyez et al., 2020)
Spadavecchia et al.	DNA hybridization	Detection limit: 0.2 nm	(Spadavecchia et al., 2013)

2.4. The observation methods of LSPR signals

To realize LSPR highly sensitive sensing detection, in addition to the optimization of the metal nanostructure, material, and modification method, the processing method of LSPR sensing signal also directly affects the sensitivity or detection limit of LSPR biosensor. Observing or collecting the LSPR signal with the binding event information is an important bridge to explore the characteristics of LSPR biosensing. Different signal processing methods for the same LSPR phenomenon may result in certain differences. Especially for the detection of very low concentration samples, the signal processing method of LSPR sensing detection becomes very important. Therefore, suitable and simple LSPR signal observation methods should be adopted reasonably for different needs.

In the above description of the means to increase the sensitivity of the biosensor, the corresponding LSPR signal observation methods are basically

To measure the shift of the LSPR resonant peak is the most common detection method. In most cases, the LSPR signal often comes from the average of multiple nanoparticles. Each nanoparticle can be used as a separate detection biosensor, which can provide a signal output with a good signal-to-noise ratio. Here, the supplemental methods of LSPR signal observation were reviewed from two aspects of darkfield detection and colorimetric biosensing.

2.4.1. Dark field microscopy (DFM) to record the LSPR testing results

For LSPR biosensing detection for ultra-sensitivity, how to distinguish the desired LSPR signal from the underlying background signal had always been a challenge that would directly affect the

results of the LSPR biosensing. However, when the observation object is from a small area or needs to reach the level of a single nanoparticle being interrogated, darkfield microscopy measurement technology based on light scattering would be very effective (D. Zhang et al., 2020), and did not require fluorescent labels and is not affected by photobleaching and blinking (Ortega-Arroyo and Kukura, 2012; Zijlstra and Orrit, 2011). Even DFM could provide resolution beyond the diffraction limit in some cases.

The darkfield microscope uses a strong and narrow beam to illuminate the sample at a high angle and then collects weak scattered light at a low angle (Chazot et al., 2020; Willets and Van Duyne, 2007). In this way, by avoiding strong and useless background signals (reflected light, transmitted light) into the eyepieces, the signal-to-noise ratio successfully increased, therefore, DFM can achieve a single particle detection level. However, as the size of the observation object is further reduced, the scattering cross-section rapidly drops with the particle diameter to the power of six (Luo et al., 2016; Weigel et al., n.d.). This makes the relatively weak scattered light weaker, and the detection contrast and sensitivity of single particles would be reduced.

The excellent light properties of precious metal nanoparticles in the scattering domain seem to make up for this: When LSPR occurs, the collective oscillation of their conduction band electrons makes the absorption band at the resonance wavelength strong, and the intensity of scattered photons far exceeds its physical cross-section (Luo et al., 2016). And the evanescent surface plasmon wave is not captured in the far-field, whereas can be scattered into a far-field mode by objects in the surface plasmon field, resulting in a dark background and bright targets. High signal-to-noise ratio and sensitivity make it develop rapidly (Gu et al., 2019). In 2019, Feng et al. prepared a silver nanoparticle coated with a thin silica layer as an internal reference (Feng et al., 2019). The introduction of this internal reference can simultaneously calibrate slow and weak reactions that are not obvious or some reactions that coexist with fast reactions. It has greatly improved the confidence level of DFM imaging analysis. Wang et al. and Gu et al. achieved high-sensitivity detection by selecting the noble metal nanoparticles of appropriate shape and combining them with DFM (Gu et al., 2019; F. Wang et al., 2019). Jin et al. applied density functional theory analysis that they analyzed the interaction of carbohydrates and proteins in real-time and high-throughput based on DFM. (Jin et al., 2015). Those experiment results illustrated that the sensitivity of DFM detection was very high. The enhancement of signal brightness and suppression of background noise were the two main factors that determine the contrast and sensitivity of DFM. In recent years, the research on improving the performance of DFM based on LSPR detection and observation has revolved around these two points or combined some data analysis and algorithm optimization. The traditional dark-field detection technology often uses a combination of a focused ring beam and a low numerical aperture objective lens to improve performance. However, the residual stray light and the low spatial resolution brought by the low numerical aperture have become obstacles hindering its development. On the other hand, although LSPR increases the intensity of scattered light, DFM is not enough to rely on intensity to identify small-sized nanoparticles in a complex noise environment. And when performing reliable analysis, a dedicated, huge microscope system or some expensive accessories are indispensable, which is not conducive to integration. Therefore, the integration of DFM devices for LSPR biosensing became an important research direction. For example, Chazot et al. proposed a luminescent photon substrate with a controlled-angle emission profile in 2020, which simplified and reduced the size of the device (Chazot et al., 2020); Sun et al. combined smartphones with

dark-field microscope analysis to create a cheap, portable and robust DFM system (Sun and Hu, 2018).

2.4.2. Colorimetric sensing based on nanoplasmonic nanoparticles

The nanoplasmonic colorimetric method is a relatively simple and reliable universal testing method in molecular diagnosis (Paterson and de la Rica, 2015; Zheng and Jiang, 2016). This method uses the color change of the detection environment caused by the occurrence of molecular binding events as the LSPR biosensor signal to transmit information to the outside. The nanoplasmonic colorimetric method usually does not require large, expensive equipment to collect, but can be easily distinguished by the naked eye with some simple conditions (King et al., 2015; Reinhard et al., 2020; Q. Zhang et al., 2020). The color change is divided into chromaticity change (a collective term for hue and saturation, indicating the type and depth of the color) and brightness change (representing the brightness of the color). In the same event, the sensitivity corresponding to different color parameters would also vary greatly (Reinhard et al., 2020). Therefore, optimizing experimental conditions and finding the best match is particularly important in nanoplasmonic colorimetric sensing. The observation methods of LSPR signal are shown in Figure 17.

In this field, the most classic case is to induce the formation of plasmonic nanoparticles by cross-linking or aggregation and control the shape or size of plasmonic nanoparticles to achieve chromaticity changes (Tang and Li, 2017). The former is to change the plasmonic coupling between the particles by inducing the aggregation and dispersion between the nanoparticles so that the color of the solution caused by the LSPR frequency shift can change visibly (Peng et al., 2014). For example, in 2015, Xianyu et al. used horseradish peroxidase (HRP) to regulate the aggregation and dispersion of gold nanoparticles (Xianyu et al., 2015). The color would change with or without HRP. The red-blue color conversion signal caused by the target at 1 ng/ml can be easily read directly by the human eye. Through precise control of the morphology or size of plasmonic nanoparticles, small differences can be easily revealed due to changes in the optical properties of LSPR (Tang and Li, 2017). For example, Zhang et al. reported an ultra-sensitive multicolor colorimetric biosensor in 2020 (Q. Zhang et al., 2020). The results illustrated that omethoate (the target detection object) can indirectly inhibit the metallization of silver ions and its concentration has a linear relationship with the shift of the nanorod LSPR peak. The detection limit of the LSPR biosensor can reach 83.2 ng/L. Since the human eye is most sensitive to blue-green, the sensing method that uses chromaticity changes as a signal is fundamental. Therefore, researchers tune the sensing peaks with narrow line width and high-intensity characteristics to the blue-green counterparts, which shown that the color changes caused by molecular binding events to be sensitively recognized by the eyes.

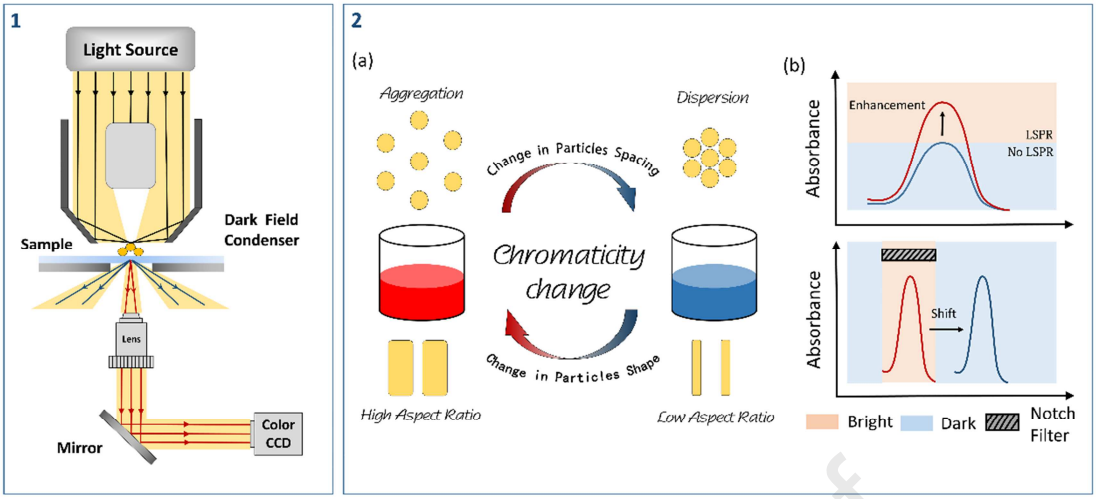

Figure 17. The observation methods of LSPR signal. **Panel (1)**. Schematic illustration of DFM. **Panel (2)**. Two signal observation methods in colorimetric sensing: (a) Chromaticity (hue and saturation) change, (b) Brightness change.

For normal humans, the sensitivity of their visual systems to changes in brightness is much higher than that of color shades. Therefore, in colorimetric sensing, the method of transmitting information through the brightness change as a signal is also very common. In 2016, Wang et al. used the LSPR excited by the nano Lycurgus cup array to enhance the electric field strength at the resonance wavelength, which greatly increased the absorbance of the dye bound to the protein (Wang et al., 2017). They extracted the light intensity from the images taken by the smartphone and normalized them with the standard color around the sample area, and obtained a detection limit close to 0.01 mg/ml through following image processing. Combined with the notch filter, there is also a sensing method based on brightness changes that can be directly observed by the human eye. Earlier, Yanik et al. obtained a resonance peak with an extremely narrow linewidth based on Fano resonance for sensing (Yanik et al., 2011). They tuned the notch filter to the band of the sensing peak, and let the notch filter block all light except the transmitted light of the sensing peak. At that time, the transmitted light of the sensing peak passed through the filter, and the CCD image was very bright. When a single layer of mouse lgG antibody to be detected was captured on the surface structure of the sensor, the sensing peak had a redshift of 22 nm, which significantly reduced the intensity of the transmitted light passing through the filter. This detection method does not require a dark environment, and can be directly observed and detected with human eyes in a routine laboratory environment.

Colorimetric sensing is a method of transforming LSPR signals into color changes that can be directly recognized by the human eye, which has the advantages of convenience, quickness, and responsiveness. However, there needs large and expensive spectroscopic detection equipment. The human eye's ability to perceive colors is uneven, therefore, colorimetric sensing can amplify the limited detection signal to a color change which can be recognized easily. It means that this method relies on a reliable signal amplification method to make the final color change sufficiently obvious. In other words, it also puts forward higher requirements for the sensitivity of contrast color sensing.

3. Conclusions and Outlook

LSPR sensors have shown great potential in the fields of portable detection and early diagnosis due to their small system size, high spectral resolution, label-free, and fast response speed. However, low sensitivity has become the main reason for limiting its application. To overcome the problem of insufficient sensitivity, many research teams have explored the issue of improving the sensitivity of LSPR sensors. Herein we review some sensitization methods from the three aspects of structure, material, and modification based on LSPR sensors and explain some related experiments. And the proceeding methods of the LSPR sensing is described from the perspective of signal observation in the end. The so-called increase of sensor sensitivity is divided into three points from the results based on spectra technology: First, the peak (or valley) value of the resonance peak (or valley) increases, the quality factor improves, and it is easier to reach the detection limit; Second, the shift of the resonance peak (or valley) increases, the changes are more obvious, and it is easier to be captured by the sensor, thereby achieving an increase in sensitivity; Third, the width of the resonance peak (or valley) is narrowed that it can improve the sensing performance. It is worth mentioning that we believe that only composite structures that combine multiple methods of sensitivity increase are the general direction of future sensitivity development. The composite structure can usually combine a variety of single sensitization methods. This leads to it being superior to other sensitization methods both in the degree of improving sensitivity and in the stability of improving sensitivity. More importantly, it can adjust the specific structural parameters according to the specific requirements in the experiment to better match the actual situation. The composite structures mentioned in this article are relatively simple. Complex ones include, for example, microfluidics, metamaterials, and biological modifications. This means that its scope of application is very wide, and it can be applied to various fields. In other words, it can be better invested in actual production practice. In the future, LSPR biosensors with high sensitivity and high sensing performance, combined with miniaturization, automation, and other latest technologies, would inevitably promote the development and progress of medical care, food inspection and other fields.

Based on the review and discussion in this paper, four important strategies to improve sensitivity are given below (shown in Figure 18).

Direction 1: Artificial intelligence assisted the design of highly sensitive LSPR sensor chip

Artificial intelligence (AI), and machine learning in particular, have fundamentally changed many aspects of science and technology, redefining the way large data sets are processed and enabling structural inferences from systems that are difficult to model. The design method of LSPR sensor chip based on machine learning and the working principle of high sensitivity sensors is designed. To understand the interaction and coupling mechanism among sensing parameters, different LSPR biosensors, and different sensing parameters, and to optimize and improve the reliability, repeatability and stability of the LSPR biosensor system and other key scientific issues. The strategy based on AI to design the LSPR chip is shown in Figure 19.

The neural network was used to analyze metal nanostructure, transmission and reflection electric field distribution, spectral structure distribution, forward and reverse pair sensing chip design. Machine learning to obtain accurate results against a large number of sensor data and simulation structures is helpful for accurate testing of cancer markers. It provides a new method and technique for the high specificity and sensitivity detection of various tumor markers in complex clinical samples.

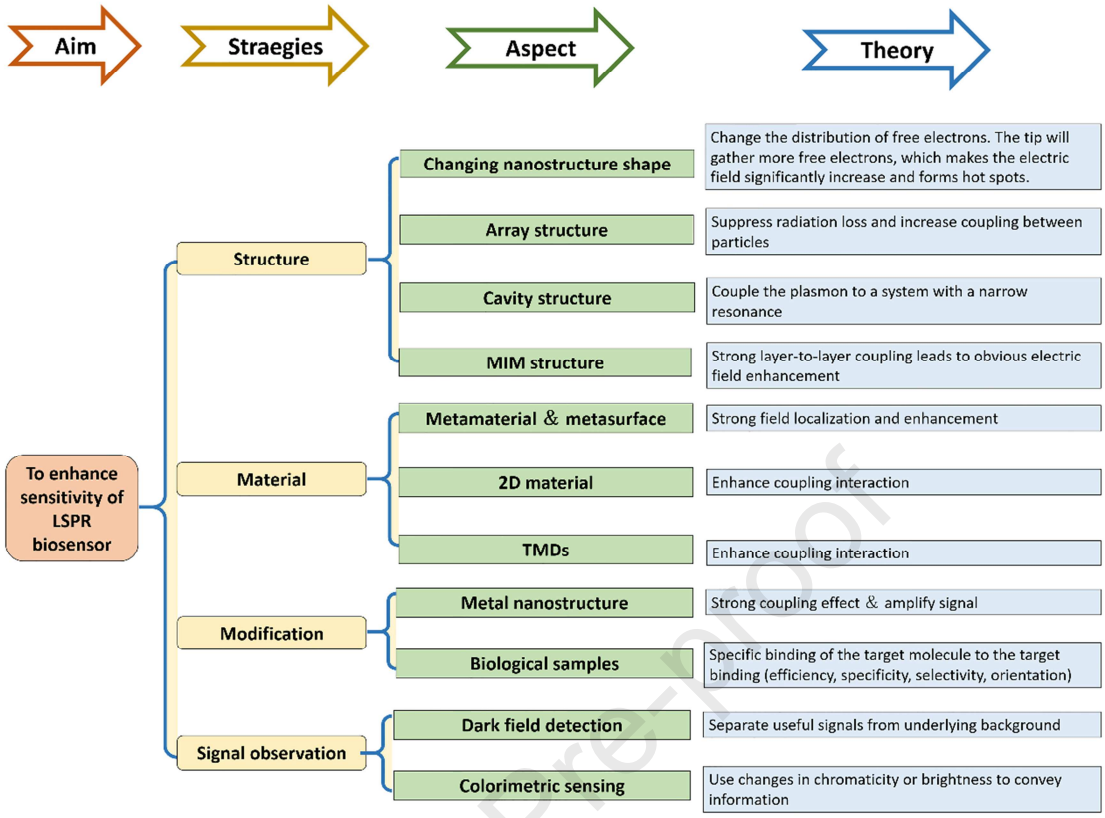

Figure 18. The methods mentioned in this article to improve the sensitivity of LSPR sensors.

Direction 2: Integrated microfluidic LSPR sensor chip

The integration of plasma and microfluidics technologies can potentially serve global health, primary care, and point-of-care (POC) applications, providing a model for affordable, robust, and portable healthcare technologies. The fusion of optical technology and the microfluidic system has a broad application prospect in the sensor field and can be used in lab-on-chip (LOC) system for darkfield, single-particle reflection and transmission spectrum measurement. Microfluidics manipulates fluids on a micro-scale to minimize the use of expensive reagents. At the same time, surface modification in a microfluidic environment can also greatly improve the binding speed between molecules, avoid all kinds of noise interference and non-specific adsorption. Moreover, cheap microchip manufacturing makes it possible to mass-produce. As sample enrichment and separation, mixing and separation function on the same chip integration, to achieve single multi-function, multi-channel, many units, many parameters, the combination of a variety of detection methods, to achieve diversity in this test should pass each other, greatly improved the detection accuracy and reliability of these features would ideally microfluidics and plasma technology together, in the POC and primary care medical solutions.

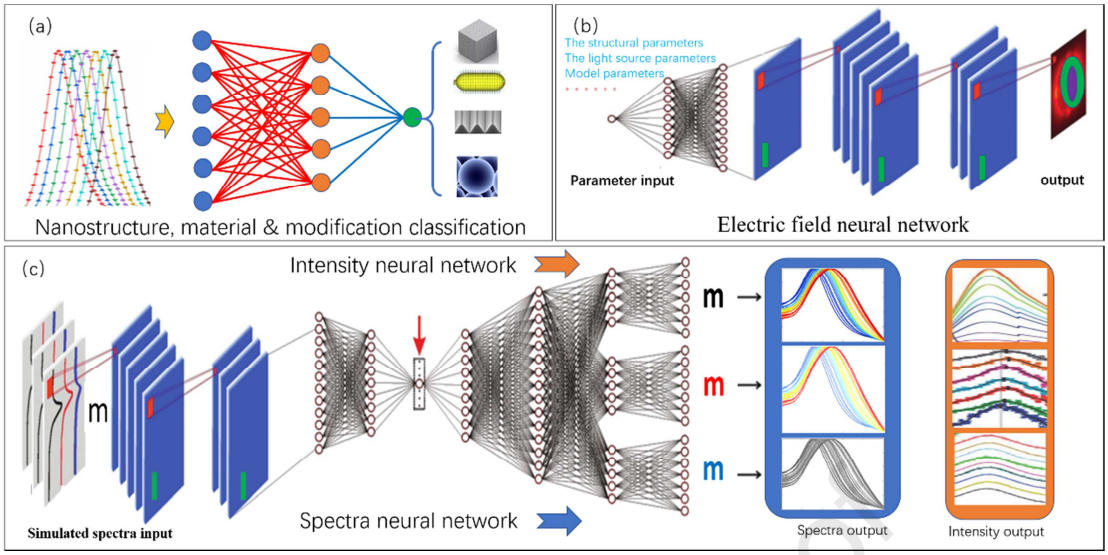

Figure 19. Machine learning for LSPR biosensor and sensing. (a) The initial populations of nanostructure geometries, material, modification method, and their calculated spectra can be used to train deep neural networks capable of predicting the spectral response of unknown designs; (b) Different parameter input into electric field neural network to obtain optimized nanostructures and spectra with high Q and sensitivity; (c) Intensity and spectra neural network was applied to get the best performances of LSPR biosensor.

Direction 3: A novel strategy for surface modification

The chemical modification and physical properties of lipid molecules enable lipid bilayers to be applied in LSPR biosensor (surface sensitive biosensor), including the detection of biomolecules, proteins, and nucleic acids. Biotinylated-lipid membranes were immobilized to detect streptavidin molecules on the surface of gold nanorods by monitoring the spectral shifts using a fast-single-particle spectroscopy instrument coupled with dark-field microscopy. Using single nanoparticles track detection method, to study the lipid-double membrane modified gold nanoparticles in molecular interactions on the cell membrane, based on membrane lipid molecules in the liquid ultrasensitive detection platform. The lipid-bilayer-incorporated biosensing platforms improve molecular interactions and form a support layer for the integration of biological cognitive elements. Therefore, this new surface functionalization strategy can be used for membrane related molecular biosensors and cancer biomarkers screening analysis.

Polymer-mediated surface functionalization is also another strategy. Polymers are used for hybridization with the plasmonic nanostructure. Meanwhile, polymers can be modified with biorecognition elements to capture target molecules, which play a key role in improving the reliability and sensitivity of biosensors. Therefore, the dynamic and functional structure of polymers can be used to develop three-dimensional binding substrates for biosensors applications.

Direction 4: High-throughput multichannel nanoplasmonic colorimetry

To improve the accuracy and reliability of LSPR detection, multiple-sample combined testing is one of the main development directions, and the testing results of multiple biological samples should be verified by each other. Multi-parameter detection of trace samples based on LSPR is mainly to realize multi-channel detection on a single LSPR chip, and the concentration of the detected samples in each channel is consistent. Meanwhile, multi-detection points (more than 10) are distributed in each channel to ensure the accidental error of testing results, thus greatly

improving the reliability of test results. If the spectral detection method is adopted, the detection speed will not be too fast. the colorimetric method or darkfield fluorescence detection method, combined with intelligent software, can realize rapid photo-taking and rapid recognition, and can realize multiple synchronous detections and obtain detection results synchronously, which has great advantages in detection speed and throughput. If combined with smart terminal devices (such as smartphones), a miniaturized mobile terminal detection system can be realized, which can be connected with the Internet to realize synchronous uploading of detection results to the network and real-time synchronous checking of detection results.

The thiol exchange process is an interesting strategy to selectively immobilize antibodies on the edges of triangular gold nanoplates that are used for the LSPR sensing platform. The thiol exchange process is an interesting strategy in which antibodies can be selectively anchored to the edges of triangular gold nanoplates used for the LSPR sensing platform. Patterning nanoplasmonic nanostructures with special geometric shapes, such as holes and edges, may be used for site-specific surface modifications, therefore, improving the practicality and specificity of nanoplasmonic platforms. To immobilize biorecognition elements. Thiol chemistry also shows wide variations in length, saturation degree, and terminal groups to better immobilize biorecognition elements (such as proteins, nucleotides, and carbohydrates) in the plasmonic active region. The thiols at the edge of the nanoplate are more easily exchanged with the thiols in solution than that at the flat surfaces due to decreased steric hindrance at high-curvature sites. In the future, this functionalization strategy would play a key role in improving sensitivity and developing multivariate analysis through specific modifications of plasma active sites. In general, surface functionalization is one of the key parameters for the development of sensitive, reliable, and accurate biosensors.

Acknowledgment

This work was supported by the National Key R&D Plan of China (2017YFB0405400), the National Natural Science Foundation of China (61774175, 61674146, 61634006 and 61875140), the Key Program of Natural Science Foundation of Beijing (4181001), and Young and Middle-aged Talents Program of the State Ethnic Affairs Commission (2019).

References

Ai, B., Basnet, P., Larson, S., Ingram, W., Zhao, Y., 2017. Plasmonic sensor with high figure of merit based on differential polarization spectra of elliptical nanohole array. Nanoscale 9, 14710–14721. https://doi.org/10.1039/C7NR06067J

Auguié, B., Barnes, W.L., 2008. Collective Resonances in Gold Nanoparticle Arrays. Phys. Rev. Lett. 101, 143902. https://doi.org/10.1103/PhysRevLett.101.143902

Averitt, R.D., Sarkar, D., Halas, N.J., 1997. Plasmon Resonance Shifts of Au-Coated Au 2 S Nanoshells: Insight into Multicomponent Nanoparticle Growth. Phys. Rev. Lett. 78, 4217–4220. https://doi.org/10.1103/PhysRevLett.78.4217

Barghouti, M.E., Akjouj, A., Mir, A., 2018. Effect of MoS2 layer on the LSPR in periodic nanostructures. Optik 171, 237–246. https://doi.org/10.1016/j.ijleo.2018.06.026

Bauch, M., Toma, K., Toma, M., Zhang, Q., Dostalek, J., 2014. Plasmon-Enhanced Fluorescence Biosensors: a Review. Plasmonics 9, 781–799. https://doi.org/10.1007/s11468-013-9660-5

Butun, S., Tongay, S., Aydin, K., 2015. Enhanced Light Emission from Large-Area Monolayer MoS_2 Using Plasmonic Nanodisc Arrays. Nano Lett. 15, 2700–2704. https://doi.org/10.1021/acs.nanolett.5b00407

Cai, J., Zhang, C., Liang, C., Min, S., Cheng, X., Li, W., 2019. Solution-Processed Large-Area Gold Nanocheckerboard Metasurfaces on Flexible Plastics for Plasmonic Biomolecular Sensing. Adv. Opt. Mater. 7, 1900516. https://doi.org/10/ghbtrc

Campion, A., Kambhampati, P., 1998. Surface-enhanced Raman scattering. Chem. Soc. Rev. 27, 241. https://doi.org/10.1039/a827241z

Cao, W., Deng, C.S., Pan, T.T., Hao, H., Wang, M., 2019a. Fabrication and sensing application of a silver nanoshell array structure by a micro-flow injection method. RSC Adv. 9, 23774–23779. https://doi.org/10.1039/C9RA03483H

Cao, W., Deng, C.S., Pan, T.T., Hao, H., Wang, M., 2019b. Fabrication and sensing application of a silver nanoshell array structure by a micro-flow injection method. RSC Adv. 9, 23774–23779. https://doi.org/10.1039/C9RA03483H

Cao, X., Ye, Y., Liu, S., 2011. Gold nanoparticle-based signal amplification for biosensing. Anal. Biochem. 417, 1–16. https://doi.org/10.1016/j.ab.2011.05.027

Cathcart, N., Chen, J.I.L., 2020. Sensing Biomarkers with Plasmonics. Anal. Chem. acs.analchem.0c00711. https://doi.org/10.1021/acs.analchem.0c00711

Cen, C., Lin, H., Huang, J., Liang, C., Chen, X., Tang, Y., Yi, Z., Ye, X., Liu, J., Yi, Y., Xiao, S., 2018a. A Tunable Plasmonic Refractive Index Sensor with Nanoring-Strip Graphene Arrays. Sensors 18, 4489. https://doi.org/10/ghbtq9

Cen, C., Lin, H., Huang, J., Liang, C., Chen, X., Tang, Y., Yi, Z., Ye, X., Liu, J., Yi, Y., Xiao, S., 2018b. A Tunable Plasmonic Refractive Index Sensor with Nanoring-Strip Graphene Arrays. Sensors 18, 4489. https://doi.org/10.3390/s18124489

Chang, C.-Y., Lin, H.-T., Lai, M.-S., Shieh, T.-Y., Peng, C.-C., Shih, M.-H., Tung, Y.-C., 2018. Flexible Localized Surface Plasmon Resonance Sensor with Metal–Insulator–Metal Nanodisks on PDMS Substrate. Sci. Rep. 8, 11812. https://doi.org/10.1038/s41598-018-30180-8

Chao, J., Cao, W., Su, S., Weng, L., Song, S., Fan, C., Wang, L., 2016. Nanostructure-based surface-enhanced Raman scattering biosensors for nucleic acids and proteins. J. Mater. Chem. B 4, 1757–1769. https://doi.org/10.1039/C5TB02135A

Chazot, C.A.C., Nagelberg, S., Rowlands, C.J., Scherer, M.R.J., Coropceanu, I., Broderick, K., Kim, Y., Bawendi, M.G., So, P.T.C., Kolle, M., 2020. Luminescent surfaces with tailored angular emission for compact dark-field imaging devices. Nat. Photonics 14, 310–315. https://doi.org/10.1038/s41566-020-0593-1

Chen, R., Huang, X., Xu, H., Xiong, Y., Li, Y., 2015. Plasmonic Enzyme-Linked Immunosorbent Assay Using Nanospherical Brushes as a Catalase Container for Colorimetric Detection of Ultralow Concentrations of *Listeria monocytogenes*. ACS Appl. Mater. Interfaces 7, 28632–28639. https://doi.org/10/f79m2z

Chen, S., Svedendahl, M., Van Duyne, R.P., Käll, M., 2011a. Plasmon-Enhanced Colorimetric ELISA with Single Molecule Sensitivity. Nano Lett. 11, 1826–1830. https://doi.org/10.1021/nl2006092

Chen, S., Svedendahl, M., Van Duyne, R.P., Käll, M., 2011b. Plasmon-Enhanced Colorimetric ELISA with Single Molecule Sensitivity. Nano Lett. 11, 1826–1830. https://doi.org/10/bgpmd2

Chen, T., 2012. Metamaterials Application in Sensing 24.

Chen, W., Hu, H., Jiang, W., Xu, Y., Zhang, S., Xu, H., 2018. Ultrasensitive nanosensors based on localized surface plasmon resonances: From theory to applications 27, 21.

Chien, M.-H., Brameshuber, M., Rossboth, B.K., Schütz, G.J., Schmid, S., 2018. Single-molecule optical absorption imaging by nanomechanical photothermal sensing. Proc. Natl. Acad. Sci. 115, 11150–11155. https://doi.org/10.1073/pnas.1804174115

Chuang, P.-C., Liao, P.-C., Chen, Y.-F., 2015. Enhancing the sensitivity of localized surface plasmon resonance (LSPR) biosensors using nanorods and DNA aptamers, in: Vo-Dinh, T., Lakowicz, J.R. (Eds.), . Presented at the SPIE BiOS, San Francisco, California, United States, p. 93400T. https://doi.org/10.1117/12.2078216

Chung, T., Lee, S.-Y., Song, E.Y., Chun, H., Lee, B., 2011. Plasmonic Nanostructures for Nano-Scale Bio-Sensing. Sensors 11, 10907–10929. https://doi.org/10.3390/s111110907

Chung, T., Lee, Y., Ahn, M.-S., Lee, W., Bae, S.-I., Hwang, C.S.H., Jeong, K.-H., 2019. Nanoislands as plasmonic materials. Nanoscale 11, 8651–8664. https://doi.org/10.1039/C8NR10539A

Cohen, L., Walt, D.R., 2019. Highly Sensitive and Multiplexed Protein Measurements. Chem. Rev. 119, 293–321. https://doi.org/10.1021/acs.chemrev.8b00257

Culver, H.R., Wechsler, M.E., Peppas, N.A., 2018. Label-Free Detection of Tear Biomarkers Using Hydrogel-Coated Gold Nanoshells in a Localized Surface Plasmon Resonance-Based Biosensor. ACS Nano 12, 9342–9354. https://doi.org/10.1021/acsnano.8b04348

Dahlin, A.B., Chen, S., Jonsson, M.P., Gunnarsson, L., Käll, M., Höök, F., 2009. High-Resolution Microspectroscopy of Plasmonic Nanostructures for Miniaturized Biosensing. Anal. Chem. 81, 6572–6580. https://doi.org/10/b6x73m

Ding, F., Wang, Z., He, S., Shalaev, V.M., Kildishev, A.V., 2015. Broadband High-Efficiency Half-Wave Plate: A Supercell-Based Plasmonic Metasurface Approach. ACS Nano 9, 4111–4119. https://doi.org/10.1021/acsnano.5b00218

Doiron, B., Mota, M., Wells, M.P., Bower, R., Mihai, A., Li, Y., Cohen, L.F., Alford, N.McN., Petrov, P.K., Oulton, R.F., Maier, S.A., 2019a. Quantifying Figures of Merit for Localized Surface Plasmon Resonance Applications: A Materials Survey. ACS Photonics 6, 240–259. https://doi.org/10.1021/acsphotonics.8b01369

Doiron, B., Mota, M., Wells, M.P., Bower, R., Mihai, A., Li, Y., Cohen, L.F., Alford, N.McN., Petrov, P.K., Oulton, R.F., Maier, S.A., 2019b. Quantifying Figures of Merit for Localized Surface Plasmon Resonance Applications: A Materials Survey. ACS Photonics 6, 240–259. https://doi.org/10/gfvxhg

Dolling, G., 2006. Simultaneous Negative Phase and Group Velocity of Light in a Metamaterial. Science 312, 892–894. https://doi.org/10.1126/science.1126021

El barghouti, M., Akjouj, A., Mir, A., 2018a. Effect of graphene layer on the localized surface plasmon resonance (LSPR) and the sensitivity in periodic nanostructure. Photonics Nanostructures - Fundam. Appl. 31, 107–114. https://doi.org/10/ghbtrb

El barghouti, M., Akjouj, A., Mir, A., 2018b. Effect of graphene layer on the localized surface plasmon resonance (LSPR) and the sensitivity in periodic nanostructure. Photonics Nanostructures - Fundam. Appl. 31, 107–114. https://doi.org/10/ghbtrb

El barghouti, M., Mir, A., Akjouj, A., Szunerits, S., 2019. Modulation of localized surface plasmon resonances of a silver nanoparticle array upon the presence of MoS2 coatings or underlying thin films. Optik 179, 819–827. https://doi.org/10.1016/j.ijleo.2018.10.208

Ertürk, G., Özen, H., Tümer, M.A., Mattiasson, B., Denizli, A., 2016. Microcontact imprinting based

surface plasmon resonance (SPR) biosensor for real-time and ultrasensitive detection of prostate specific antigen (PSA) from clinical samples. Sens. Actuators B Chem. 224, 823–832. https://doi.org/10.1016/j.snb.2015.10.093

Escobedo, C., 2013. On-chip nanohole array based sensing: a review. Lab. Chip 13, 2445. https://doi.org/10.1039/c3lc50107h

Fang, Z., Cai, J., Yan, Z., Nordlander, P., Halas, N.J., Zhu, X., 2011. Removing a Wedge from a Metallic Nanodisk Reveals a Fano Resonance. Nano Lett. 11, 4475–4479. https://doi.org/10/bkhzzw

Feng, W., He, W., Zhou, J., Gu, X.Y., Li, Y.F., Huang, C.Z., 2019. Inconspicuous Reactions Identified by Improved Precision of Plasmonic Scattering Dark-Field Microscopy Imaging Using Silver Shell-Isolated Nanoparticles as Internal References. Anal. Chem. 91, 3002–3008. https://doi.org/10.1021/acs.analchem.8b05285

Fleischmann, M., Hendra, P.J., McQUILLAN, A.J., n.d. RAMAN SPECTRA OF PYRIDZNE ADSORBED AT A SILVER ELECTRODE. Chem. Phys. Lett. 26, 4.

Gan, C.H., Chu, H.S., Li, E.P., 2012. Synthesis of highly confined surface plasmon modes with doped graphene sheets in the midinfrared and terahertz frequencies. Phys. Rev. B 85, 125431. https://doi.org/10.1103/PhysRevB.85.125431

Gao, Y., Zhou, Y., Chandrawati, R., 2020. Metal and Metal Oxide Nanoparticles to Enhance the Performance of Enzyme-Linked Immunosorbent Assay (ELISA). ACS Appl. Nano Mater. 3, 1–21. https://doi.org/10/ghbtrj

Ghobadi, A., Hajian, H., Gokbayrak, M., Dereshgi, S.A., Toprak, A., Butun, B., Ozbay, E., 2017. Visible light nearly perfect absorber: an optimum unit cell arrangement for near absolute polarization insensitivity. Opt. Express 25, 27624. https://doi.org/10.1364/OE.25.027624

Glybovski, S.B., Tretyakov, S.A., Belov, P.A., Kivshar, Y.S., Simovski, C.R., 2016. Metasurfaces: From microwaves to visible. Phys. Rep. 634, 1–72. https://doi.org/10.1016/j.physrep.2016.04.004

Gu, X.Y., Liu, J.J., Gao, P.F., Li, Y.F., Huang, C.Z., 2019. Gold Triangular Nanoplates Based Single-Particle Dark-Field Microscopy Assay of Pyrophosphate. Anal. Chem. 91, 15798–15803. https://doi.org/10.1021/acs.analchem.9b04093

Ha, M., Kim, J.-H., You, M., Li, Q., Fan, C., Nam, J.-M., 2019. Multicomponent Plasmonic Nanoparticles: From Heterostructured Nanoparticles to Colloidal Composite Nanostructures. Chem. Rev. 119, 12208–12278. https://doi.org/10.1021/acs.chemrev.9b00234

Hackett, L.P., Ameen, A., Li, W., Dar, F.K., Goddard, L.L., Liu, G.L., 2018. Spectrometer-Free Plasmonic Biosensing with Metal–Insulator–Metal Nanocup Arrays. ACS Sens. 3, 290–298. https://doi.org/10/ghbtrd

Haes, A.J., Van Duyne, R.P., 2002. A Nanoscale Optical Biosensor: Sensitivity and Selectivity of an Approach Based on the Localized Surface Plasmon Resonance Spectroscopy of Triangular Silver Nanoparticles. J. Am. Chem. Soc. 124, 10596–10604. https://doi.org/10/b2hgtw

Hall, W.P., Ngatia, S.N., Van Duyne, R.P., 2011. LSPR Biosensor Signal Enhancement Using Nanoparticle−Antibody Conjugates. J. Phys. Chem. C 115, 1410–1414. https://doi.org/10/crq9dp

Hanarp, P., Käll, M., Sutherland, D.S., 2003. Optical Properties of Short Range Ordered Arrays of Nanometer Gold Disks Prepared by Colloidal Lithography. J. Phys. Chem. B 107, 5768–

5772. https://doi.org/10.1021/jp027562k

Hasan, D., Ho, C.P., Pitchappa, P., Lee, C., 2015. Dipolar Resonance Enhancement and Magnetic Resonance in Cross-Coupled Bow-Tie Nanoantenna Array by Plasmonic Cavity. ACS Photonics 2, 890–898. https://doi.org/10.1021/acsphotonics.5b00088

Hirsch, L.R., Jackson, J.B., Lee, A., Halas, N.J., West, J.L., 2003. A Whole Blood Immunoassay Using Gold Nanoshells. Anal. Chem. 75, 2377–2381. https://doi.org/10.1021/ac0262210

Hoffman, A.J., Alekseyev, L., Howard, S.S., Franz, K.J., Wasserman, D., Podolskiy, V.A., Narimanov, E.E., Sivco, D.L., Gmachl, C., 2007. Negative refraction in semiconductor metamaterials. Nat. Mater. 6, 946–950. https://doi.org/10.1038/nmat2033

Homola, J., n.d. Surface Plasmon Resonance Sensors for Detection of Chemical and Biological Species 32.

Hong, X., Hall, E.A.H., 2012. Contribution of gold nanoparticles to the signal amplification in surface plasmon resonance. The Analyst 137, 4712. https://doi.org/10.1039/c2an35742a

Hu, L., Huang, Y., Fang, L., Chen, G., Wei, H., Fang, Y., 2015. Fano resonance assisting plasmonic circular dichroism from nanorice heterodimers for extrinsic chirality. Sci. Rep. 5, 16069. https://doi.org/10.1038/srep16069

Huang, J.-Y., Lin, H.-T., Chen, T.-H., Chen, C.-A., Chang, H.-T., Chen, C.-F., 2018. Signal Amplified Gold Nanoparticles for Cancer Diagnosis on Paper-Based Analytical Devices. ACS Sens. 3, 174–182. https://doi.org/10.1021/acssensors.7b00823

Huang, W.-X., Guo, J.-J., Wang, M.-S., Zhao, G.-R., 2017. Sensor based on Fano resonances of plane metamaterial with narrow slits. Phys. Lett. A 381, 909–912. https://doi.org/10.1016/j.physleta.2017.01.005

Huang, Y., Zhang, X., Ringe, E., Hou, M., Ma, L., Zhang, Z., 2016. Tunable Lattice Coupling of Multipole Plasmon Modes and Near-Field Enhancement in Closely Spaced Gold Nanorod Arrays. Sci. Rep. 6, 23159. https://doi.org/10.1038/srep23159

Inverted Size-Dependence of Surface-Enhanced Raman Scattering on Gold Nanohole and Nanodisk Arrays | Nano Letters [WWW Document], n.d. URL https://doi.org/10.1021/nl0806163 (accessed 8.6.20).

J. Scheue, n.d. Optical Metasurfaces Are Coming of Age: Short- and Long-Term Opportunities for Commercial Applications | ACS Photonics [WWW Document]. URL https://doi.org/10.1021/acsphotonics.9b01719 (accessed 8.23.20).

Jensen, T.R., Duval, M.L., Kelly, K.L., Lazarides, A.A., Schatz, G.C., Van Duyne, R.P., 1999. Nanosphere Lithography: Effect of the External Dielectric Medium on the Surface Plasmon Resonance Spectrum of a Periodic Array of Silver Nanoparticles. J. Phys. Chem. B 103, 9846–9853. https://doi.org/10/bpx9qw

Jia, P., Jiang, H., Sabarinathan, J., Yang, J., 2013. Plasmonic nanohole array sensors fabricated by template transfer with improved optical performance. Nanotechnology 24, 195501. https://doi.org/10.1088/0957-4484/24/19/195501

Jia, P., Kong, D., Ebendorff-Heidepriem, H., 2020. Flexible Plasmonic Tapes with Nanohole and Nanoparticle Arrays for Refractometric and Strain Sensing. ACS Appl. Nano Mater. acsanm.0c01673. https://doi.org/10.1021/acsanm.0c01673

Jin, H.-Y., Li, D.-W., Zhang, N., Gu, Z., Long, Y.-T., 2015. Analyzing Carbohydrate–Protein Interaction Based on Single Plasmonic Nanoparticle by Conventional Dark Field Microscopy. ACS Appl. Mater. Interfaces 7, 12249–12253. https://doi.org/10.1021/acsami.5b02744

Jo, S., Lee, W., Park, Joohyung, Kim, Woong, Kim, Woochang, Lee, G., Lee, H.-J., Hong, J., Park, Jinsung, 2020. Localized surface plasmon resonance aptasensor for the highly sensitive direct detection of cortisol in human saliva. Sens. Actuators B Chem. 304, 127424. https://doi.org/10.1016/j.snb.2019.127424

Jung, L.S., Campbell, C.T., Chinowsky, T.M., Mar, M.N., Yee, S.S., 1998. Quantitative Interpretation of the Response of Surface Plasmon Resonance Sensors to Adsorbed Films. Langmuir 14, 5636–5648. https://doi.org/10.1021/la971228b

Jung, Y., Hwang, I., Yu, J., Lee, Jihye, Choi, J.-H., Jeong, J.-H., Jung, J.-Y., Lee, Jongwon, 2019. Fano Metamaterials on Nanopedestals for Plasmon-Enhanced Infrared Spectroscopy. Sci. Rep. 9, 7834. https://doi.org/10.1038/s41598-019-44396-9

Kaewwonglom, N., Oliver, M., Cocovi-Solberg, D.J., Zirngibl, K., Knopp, D., Jakmunee, J., Miró, M., 2019. Reliable Sensing Platform for Plasmonic Enzyme-Linked Immunosorbent Assays Based on Automatic Flow-Based Methodology. Anal. Chem. 91, 13260–13267. https://doi.org/10/ghbtrh

Kalia, J., Raines, R., 2010. Advances in Bioconjugation. Curr. Org. Chem. 14, 138–147. https://doi.org/10.2174/138527210790069839

Kang, T.Y., Lee, W., Ahn, H., Shin, D.-M., Kim, C.-S., Oh, J.-W., Kim, D., Kim, K., 2017. Plasmon-Coupled Whispering Gallery Modes on Nanodisk Arrays for Signal Enhancements. Sci. Rep. 7, 11737. https://doi.org/10.1038/s41598-017-12053-8

Kaul, A.B., 2014. Two-dimensional layered materials: Structure, properties, and prospects for device applications. J. Mater. Res. 29, 348–361. https://doi.org/10.1557/jmr.2014.6

Khateb, H., Klös, G., Meyer, R.L., Sutherland, D.S., 2020a. Development of a Label-Free LSPR-Apta Sensor for Staphylococcus aureus Detection. ACS Appl. Bio Mater. https://doi.org/10/gg9rs6

Khateb, H., Klös, G., Meyer, R.L., Sutherland, D.S., 2020b. Development of a Label-Free LSPR-Apta Sensor for *Staphylococcus aureus* Detection. ACS Appl. Bio Mater. 3, 3066–3077. https://doi.org/10.1021/acsabm.0c00110

King, N.S., Liu, L., Yang, X., Cerjan, B., Everitt, H.O., Nordlander, P., Halas, N.J., 2015. Fano Resonant Aluminum Nanoclusters for Plasmonic Colorimetric Sensing. ACS Nano 9, 10628–10636. https://doi.org/10.1021/acsnano.5b04864

Ko, W., Chang, C., Chiang, Y., Huang, Li-Ting, Huang, Lih-Wen, Lin, K., 2019a. Immunoassay of plasmonic gold-nanoparticle clusters: Plasmon coupling effects for Parkinson biomarker detection. J. Chin. Chem. Soc. 66, 982–987. https://doi.org/10.1002/jccs.201900072

Ko, W., Chang, C., Chiang, Y., Huang, Li-Ting, Huang, Lih-Wen, Lin, K., 2019b. Immunoassay of plasmonic gold-nanoparticle clusters: Plasmon coupling effects for Parkinson biomarker detection. J. Chin. Chem. Soc. 66, 982–987. https://doi.org/10/ghbtrk

Koppens, F.H.L., Chang, D.E., García de Abajo, F.J., 2011. Graphene Plasmonics: A Platform for Strong Light–Matter Interactions. Nano Lett. 11, 3370–3377. https://doi.org/10.1021/nl201771h

Kravets, V.G., Kabashin, A.V., Barnes, W.L., Grigorenko, A.N., 2018. Plasmonic Surface Lattice Resonances: A Review of Properties and Applications. Chem. Rev. 118, 5912–5951. https://doi.org/10.1021/acs.chemrev.8b00243

Kwon, J.A., Jin, C.M., Shin, Y., Kim, H.Y., Kim, Y., Kang, T., Choi, I., 2018. Tunable Plasmonic Cavity for Label-free Detection of Small Molecules. ACS Appl. Mater. Interfaces 10, 13226–

13235. https://doi.org/10.1021/acsami.8b01550

Langer, J., Jimenez de Aberasturi, D., Aizpurua, J., Alvarez-Puebla, R.A., Auguié, B., Baumberg, J.J., Bazan, G.C., Bell, S.E.J., Boisen, A., Brolo, A.G., Choo, J., Cialla-May, D., Deckert, V., Fabris, L., Faulds, K., García de Abajo, F.J., Goodacre, R., Graham, D., Haes, A.J., Haynes, C.L., Huck, C., Itoh, T., Käll, M., Kneipp, J., Kotov, N.A., Kuang, H., Le Ru, E.C., Lee, H.K., Li, J.-F., Ling, X.Y., Maier, S.A., Mayerhöfer, T., Moskovits, M., Murakoshi, K., Nam, J.-M., Nie, S., Ozaki, Y., Pastoriza-Santos, I., Perez-Juste, J., Popp, J., Pucci, A., Reich, S., Ren, B., Schatz, G.C., Shegai, T., Schlücker, S., Tay, L.-L., Thomas, K.G., Tian, Z.-Q., Van Duyne, R.P., Vo-Dinh, T., Wang, Y., Willets, K.A., Xu, C., Xu, H., Xu, Y., Yamamoto, Y.S., Zhao, B., Liz-Marzán, L.M., 2020. Present and Future of Surface-Enhanced Raman Scattering. ACS Nano 14, 28–117. https://doi.org/10.1021/acsnano.9b04224

Langer, J., Novikov, S.M., Liz-Marzán, L.M., 2015. Sensing using plasmonic nanostructures and nanoparticles. Nanotechnology 26, 322001. https://doi.org/10.1088/0957-4484/26/32/322001

Lee, J.E., Seo, J.H., Kim, C.S., Kwon, Y., Ha, J.H., Choi, S.S., Cha, H.J., 2013. A comparative study on antibody immobilization strategies onto solid surface. Korean J Chem Eng 30, 5.

Lee, S.-W., Lee, K.-S., Ahn, J., Lee, J.-J., Kim, M.-G., Shin, Y.-B., 2011. Highly Sensitive Biosensing Using Arrays of Plasmonic Au Nanodisks Realized by Nanoimprint Lithography. ACS Nano 5, 897–904. https://doi.org/10.1021/nn102041m

Leidner, L., Stäb, J., Adam, J.T., Gauglitz, G., 2016. Surface-enhanced infrared absorption studies towards a new optical biosensor. Beilstein J. Nanotechnol. 7, 1736–1742. https://doi.org/10.3762/bjnano.7.166

Lesuffleur, A., Im, H., Lindquist, N.C., Oh, S.-H., 2007. Periodic nanohole arrays with shape-enhanced plasmon resonance as real-time biosensors. Appl. Phys. Lett. 90, 243110. https://doi.org/10.1063/1.2747668

Li, H., Wu, J., Yin, Z., Zhang, H., 2014. Preparation and Applications of Mechanically Exfoliated Single-Layer and Multilayer MoS_2 and WSe_2 Nanosheets. Acc. Chem. Res. 47, 1067–1075. https://doi.org/10.1021/ar4002312

Liang, Y., Zhang, H., Zhu, W., Agrawal, A., Lezec, H., Li, L., Peng, W., Zou, Y., Lu, Y., Xu, T., 2017. Subradiant Dipolar Interactions in Plasmonic Nanoring Resonator Array for Integrated Label-Free Biosensing. ACS Sens. 2, 1796–1804. https://doi.org/10.1021/acssensors.7b00607

Liang, Zhaokang, Wen, Y., Zhang, Z., Liang, Zihao, Xu, Z., Lin, Y.-S., 2019. Plasmonic metamaterial using metal-insulator-metal nanogratings for high-sensitive refraction index sensor. Results Phys. 15, 102602. https://doi.org/10/gg9rs5

Limonov, M.F., Rybin, M.V., Poddubny, A.N., Kivshar, Y.S., 2017. Fano resonances in photonics. Nat. Photonics 11, 543–554. https://doi.org/10.1038/nphoton.2017.142

Liu, G.-S., Xiong, X., Hu, S., Shi, W., Chen, Y., Zhu, W., Zheng, H., Yu, J., Azeman, N.H., Luo, Y., Chen, Z., n.d. Photonic cavity enhanced high-performance surface plasmon resonance biosensor 9.

Liu, J., Jalali, M., Mahshid, S., Wachsmann-Hogiu, S., 2020. Are plasmonic optical biosensors ready for use in point-of-need applications? The Analyst 145, 364–384. https://doi.org/10.1039/C9AN02149C

Liu, N., Weiss, T., Mesch, M., Langguth, L., Eigenthaler, U., Hirscher, M., Sönnichsen, C., Giessen,

H., 2010. Planar Metamaterial Analogue of Electromagnetically Induced Transparency for Plasmonic Sensing. Nano Lett. 10, 1103–1107. https://doi.org/10.1021/nl902621d

Liu, W., Lee, B., Naylor, C.H., Ee, H.-S., Park, J., Johnson, A.T.C., Agarwal, R., 2016. Strong Exciton–Plasmon Coupling in MoS $_2$ Coupled with Plasmonic Lattice. Nano Lett. 16, 1262–1269. https://doi.org/10.1021/acs.nanolett.5b04588

Loyez, M., Hassan, E.M., Lobry, M., Liu, F., Caucheteur, C., Wattiez, R., DeRosa, M.C., Willmore, W.G., Albert, J., 2020. Rapid Detection of Circulating Breast Cancer Cells Using a Multiresonant Optical Fiber Aptasensor with Plasmonic Amplification. ACS Sens. 5, 454–463. https://doi.org/10.1021/acssensors.9b02155

Lu, H., Gan, X., Mao, D., Jia, B., Zhao, J., 2018. Flexibly tunable high-quality-factor induced transparency in plasmonic systems. Sci. Rep. 8, 1558. https://doi.org/10.1038/s41598-018-19869-y

Lu, W.B., Zhu, W., Xu, H.J., Ni, Z.H., Dong, Z.G., Cui, T.J., 2013. Flexible transformation plasmonics using graphene. Opt. Express 21, 10475. https://doi.org/10.1364/OE.21.010475

Lu, Y., Liu, G.L., Kim, J., Mejia, Y.X., Lee, L.P., 2005. Nanophotonic Crescent Moon Structures with Sharp Edge for Ultrasensitive Biomolecular Detection by Local Electromagnetic Field Enhancement Effect. Nano Lett. 5, 119–124. https://doi.org/10/dz7k2s

Luo, W., Wu, M., Li, S., Xu, Y., Ye, Z., Wei, L., Chen, B., Xu, Q.-H., Xiao, L., 2016. Nanoprecipitation of Fluorescent Conjugated Polymer onto the Surface of Plasmonic Nanoparticle for Fluorescence/Dark-Field Dual-Modality Single Particle Imaging. Anal. Chem. 88, 6827–6835. https://doi.org/10.1021/acs.analchem.6b01350

Marae-Djouda, J., Gontier, A., Caputo, R., Lévêque, G., Bercu, B., Madi, Y., Montay, G., Adam, P.-M., Molinari, M., Stagon, S., Maurer, T., 2018. Dense Brushes of Tilted Metallic Nanorods Grown onto Stretchable Substrates for Optical Strain Sensing. ACS Appl. Nano Mater. 1, 2347–2355. https://doi.org/10.1021/acsanm.8b00441

Masson, J.-F., 2017. Surface Plasmon Resonance Clinical Biosensors for Medical Diagnostics. ACS Sens. 2, 16–30. https://doi.org/10.1021/acssensors.6b00763

Mehrotra, P., 2016. Biosensors and their applications – A review. J. Oral Biol. Craniofacial Res. 6, 153–159. https://doi.org/10.1016/j.jobcr.2015.12.002

Nan, J., Zhu, S., Ye, S., Sun, W., Yue, Y., Tang, X., Shi, J., Xu, X., Zhang, J., Yang, B., 2020. Ultrahigh-Sensitivity Sandwiched Plasmon Ruler for Label-Free Clinical Diagnosis. Adv. Mater. 32, 1905927. https://doi.org/10.1002/adma.201905927

Narasimhan, V., Siddique, R.H., Park, H., Choo, H., 2020. Bioinspired Disordered Flexible Metasurfaces for Human Tear Analysis Using Broadband Surface-Enhanced Raman Scattering. ACS Omega 5, 12915–12922. https://doi.org/10/ghbtrf

Nehl, C.L., Liao, H., Hafner, J.H., 2006. Optical Properties of Star-Shaped Gold Nanoparticles. Nano Lett. 6, 683–688. https://doi.org/10.1021/nl052409y

Niu, L.-Y., Wang, Q., Zhao, W.-M., Jing, J.-Y., 2020. High quality factor D-type fiber surface plasmon resonance (SPR) sensor based on the modification of gold nanoshells. Instrum. Sci. Technol. 48, 63–74. https://doi.org/10.1080/10739149.2019.1655762

Nunna, B.B., 2019. Detection of cancer antigens (CA-125) using gold nano particles on interdigitated electrode-based microfluidic biosensor 12. https://doi.org/10/ggqv6s

Oliverio, M., Perotto, S., Messina, G.C., Lovato, L., De Angelis, F., 2017a. Chemical Functionalization of Plasmonic Surface Biosensors: A Tutorial Review on Issues,

Strategies, and Costs. ACS Appl. Mater. Interfaces 9, 29394–29411. https://doi.org/10.1021/acsami.7b01583

Oliverio, M., Perotto, S., Messina, G.C., Lovato, L., De Angelis, F., 2017b. Chemical Functionalization of Plasmonic Surface Biosensors: A Tutorial Review on Issues, Strategies, and Costs. ACS Appl. Mater. Interfaces 9, 29394–29411. https://doi.org/10.1021/acsami.7b01583

Ortega-Arroyo, J., Kukura, P., 2012. Interferometric scattering microscopy (iSCAT): new frontiers in ultrafast and ultrasensitive optical microscopy. Phys. Chem. Chem. Phys. 14, 15625. https://doi.org/10.1039/c2cp41013c

Palermo, G., Lio, G.E., Esposito, M., Ricciardi, L., Manoccio, M., Tasco, V., Passaseo, A., De Luca, A., Strangi, G., 2020. Biomolecular Sensing at the Interface between Chiral Metasurfaces and Hyperbolic Metamaterials. ACS Appl. Mater. Interfaces 12, 30181–30188. https://doi.org/10.1021/acsami.0c07415

Paria, D., Zhang, C., Barman, I., 2019. Towards rational design and optimization of near-field enhancement and spectral tunability of hybrid core-shell plasmonic nanoprobes. Sci. Rep. 9, 16071. https://doi.org/10.1038/s41598-019-52418-9

Park, Y.I., Im, H., Weissleder, R., Lee, H., 2015. Nanostar Clustering Improves the Sensitivity of Plasmonic Assays. Bioconjug. Chem. 26, 1470–1474. https://doi.org/10.1021/acs.bioconjchem.5b00343

Paterson, S., de la Rica, R., 2015. Solution-based nanosensors for in-field detection with the naked eye. The Analyst 140, 3308–3317. https://doi.org/10.1039/C4AN02297A

Peng, C., Duan, X., Khamba, G.W., Xie, Z., 2014. Highly sensitive “signal on” plasmonic ELISA for small molecules by the naked eye. Anal Methods 6, 9616–9621. https://doi.org/10.1039/C4AY01993H

Pita, M., Cui, L., Gaikwad, R.M., Katz, E., Sokolov, I., 2008. High sensitivity molecular detection with enzyme-linked immuno-sorbent assay (ELISA)-type immunosensing. Nanotechnology 19, 375502. https://doi.org/10.1088/0957-4484/19/37/375502

Prikulis, J., Hanarp, P., Olofsson, L., Sutherland, D., Käll, M., 2004. Optical Spectroscopy of Nanometric Holes in Thin Gold Films. Nano Lett. 4, 1003–1007. https://doi.org/10.1021/nl0497171

Reimhult, E., Höök, F., 2015. Design of Surface Modifications for Nanoscale Sensor Applications. Sensors 15, 1635–1675. https://doi.org/10.3390/s150101635

Reinhard, I., Miller, K., Diepenheim, G., Cantrell, K., Hall, W.P., 2020. Nanoparticle Design Rules for Colorimetric Plasmonic Sensors. ACS Appl. Nano Mater. 3, 4342–4350. https://doi.org/10.1021/acsanm.0c00475

Rindzevicius, T., Alaverdyan, Y., Dahlin, A., Höök, F., Sutherland, D.S., Käll, M., 2005. Plasmonic Sensing Characteristics of Single Nanometric Holes. Nano Lett. 5, 2335–2339. https://doi.org/10.1021/nl0516355

Rissin, D.M., n.d. CHAPTER 2.13 - Measurement of Single Protein Molecules Using Digital ELISA. Immunoass. Handb. 20.

Sagle, L.B., Ruvuna, L.K., Ruemmele, J.A., Van Duyne, R.P., 2011. Advances in localized surface plasmon resonance spectroscopy biosensing. Nanomed. 6, 1447–1462. https://doi.org/10/dzc59c

Saha, K., Agasti, S.S., Kim, C., Li, X., Rotello, V.M., 2012. Gold Nanoparticles in Chemical and

Biological Sensing. Chem. Rev. 112, 2739–2779. https://doi.org/10.1021/cr2001178

Sherry, L.J., Jin, R., Mirkin, C.A., Schatz, G.C., Van Duyne, R.P., 2006. Localized Surface Plasmon Resonance Spectroscopy of Single Silver Triangular Nanoprisms. Nano Lett. 6, 2060–2065. https://doi.org/10/b7dhjx

Shumaker-Parry, J.S., Rochholz, H., Kreiter, M., 2005. Fabrication of Crescent-Shaped Optical Antennas. Adv. Mater. 17, 2131–2134. https://doi.org/10/brf797

Siddique, R.H., Kumar, S., Narasimhan, V., Kwon, H., Choo, H., 2019. Aluminum Metasurface with Hybrid Multipolar Plasmons for 1000-Fold Broadband Visible Fluorescence Enhancement and Multiplexed Biosensing. ACS Nano 13, 13775–13783. https://doi.org/10.1021/acsnano.9b02926

Smith, D.R., 2004. Metamaterials and Negative Refractive Index. Science 305, 788–792. https://doi.org/10.1126/science.1096796

Song, H., Zhang, H., Sun, Z., Ren, Z., Yang, X., Wang, Q., 2019. Triangular silver nanoparticle U-bent fiber sensor based on localized surface plasmon resonance. AIP Adv. 9, 085307. https://doi.org/10.1063/1.5111820

Sönnichsen, C., Reinhard, B.M., Liphardt, J., Alivisatos, A.P., 2005. A molecular ruler based on plasmon coupling of single gold and silver nanoparticles. Nat. Biotechnol. 23, 741–745. https://doi.org/10.1038/nbt1100

Spadavecchia, J., Barras, A., Lyskawa, J., Woisel, P., Laure, W., Pradier, C.-M., Boukherroub, R., Szunerits, S., 2013. Approach for Plasmonic Based DNA Sensing: Amplification of the Wavelength Shift and Simultaneous Detection of the Plasmon Modes of Gold Nanostructures. Anal. Chem. 85, 3288–3296. https://doi.org/10.1021/ac3036316

Sreekanth, K.V., Alapan, Y., ElKabbash, M., Ilker, E., Hinczewski, M., Gurkan, U.A., De Luca, A., Strangi, G., 2016a. Extreme sensitivity biosensing platform based on hyperbolic metamaterials. Nat. Mater. 15, 621–627. https://doi.org/10.1038/nmat4609

Sreekanth, K.V., ElKabbash, M., Alapan, Y., Ilker, E.I., Hinczewski, M., Gurkan, U.A., Strangi, G., 2017. Hyperbolic metamaterials-based plasmonic biosensor for fluid biopsy with single molecule sensitivity. EPJ Appl. Metamaterials 4, 1. https://doi.org/10.1051/epjam/2016015

Sreekanth, K.V., ElKabbash, M., Alapan, Y., Rashed, A.R., Gurkan, U.A., Strangi, G., 2016b. A multiband perfect absorber based on hyperbolic metamaterials. Sci. Rep. 6, 26272. https://doi.org/10.1038/srep26272

Sun, D., Hu, T.Y., 2018. A low cost mobile phone dark-field microscope for nanoparticle-based quantitative studies. Biosens. Bioelectron. 99, 513–518. https://doi.org/10.1016/j.bios.2017.08.025

Sun, Y., Xia, Y., 2002. Increased Sensitivity of Surface Plasmon Resonance of Gold Nanoshells Compared to That of Gold Solid Colloids in Response to Environmental Changes. Anal. Chem. 74, 5297–5305. https://doi.org/10.1021/ac0258352

Takei, H., Bessho, N., Ishii, A., Okamoto, T., Beyer, A., Vieker, H., Gölzhäuser, A., 2014. Enhanced Infrared LSPR Sensitivity of Cap-Shaped Gold Nanoparticles Coupled to a Metallic Film. Langmuir 30, 2297–2305. https://doi.org/10.1021/la403407g

Tam, F., Moran, C., Halas, N., 2004. Geometrical Parameters Controlling Sensitivity of Nanoshell Plasmon Resonances to Changes in Dielectric Environment. J. Phys. Chem. B 108, 17290–17294. https://doi.org/10.1021/jp048499x

Tang, L., Li, J., 2017. Plasmon-Based Colorimetric Nanosensors for Ultrasensitive Molecular Diagnostics. ACS Sens. 2, 857–875. https://doi.org/10.1021/acssensors.7b00282

Tang, Q., Zhou, Z., 2013. Graphene-analogous low-dimensional materials. Prog. Mater. Sci. 58, 1244–1315. https://doi.org/10.1016/j.pmatsci.2013.04.003

Tao, H., Strikwerda, A.C., Liu, M., Mondia, J.P., Ekmekci, E., Fan, K., Kaplan, D.L., Padilla, W.J., Zhang, X., Averitt, R.D., Omenetto, F.G., 2010. Performance enhancement of terahertz metamaterials on ultrathin substrates for sensing applications. Appl. Phys. Lett. 97, 261909. https://doi.org/10.1063/1.3533367

Tittl, A., John-Herpin, A., Leitis, A., Arvelo, E.R., Altug, H., 2019. Metasurface-Based Molecular Biosensing Aided by Artificial Intelligence. Angew. Chem. Int. Ed. 58, 14810–14822. https://doi.org/10.1002/anie.201901443

Tobing, L.Y.M., Tjahjana, L., Zhang, D.H., Zhang, Q., Xiong, Q., n.d. Deep subwavelength fourfold rotationally symmetric split-ring-resonator metamaterials for highly sensitive and robust biosensing platform. Sci. Rep. 6.

Tokel, O., Inci, F., Demirci, U., 2014a. Advances in Plasmonic Technologies for Point of Care Applications. Chem. Rev. 114, 5728–5752. https://doi.org/10.1021/cr4000623

Tokel, O., Inci, F., Demirci, U., 2014b. Advances in Plasmonic Technologies for Point of Care Applications. Chem. Rev. 114, 5728–5752. https://doi.org/10.1021/cr4000623

Tsai, C.-Y., Lu, S.-P., Lin, J.-W., Lee, P.-T., 2011. High sensitivity plasmonic index sensor using slablike gold nanoring arrays. Appl. Phys. Lett. 98, 153108. https://doi.org/10/chpcjv

Vashist, S.K., Lam, E., Hrapovic, S., Male, K.B., Luong, J.H.T., 2014. Immobilization of Antibodies and Enzymes on 3-Aminopropyltriethoxysilane-Functionalized Bioanalytical Platforms for Biosensors and Diagnostics. Chem. Rev. 114, 11083–11130. https://doi.org/10.1021/cr5000943

Wang, B.-X., Zhai, X., Wang, G.-Z., Huang, W.-Q., Wang, L.-L., 2015. A novel dual-band terahertz metamaterial absorber for a sensor application. J. Appl. Phys. 117, 014504. https://doi.org/10.1063/1.4905261

Wang, F., Li, Y., Han, Y., Ye, Z., Wei, L., Luo, H.-B., Xiao, L., 2019. Single-Particle Enzyme Activity Assay with Spectral-Resolved Dark-Field Optical Microscopy. Anal. Chem. 91, 6329–6339. https://doi.org/10.1021/acs.analchem.9b01300

Wang, F., Zhang, Y., Tian, C., Girit, C., Zettl, A., Crommie, M., Shen, Y.R., 2008. Gate-Variable Optical Transitions in Graphene. Science 320, 206–209. https://doi.org/10.1126/science.1152793

Wang, H., Brandl, D.W., Le, F., Nordlander, P., Halas, N.J., 2006. Nanorice: A Hybrid Plasmonic Nanostructure. Nano Lett. 6, 827–832. https://doi.org/10.1021/nl060209w

Wang, J., Duan, G., Li, Y., Liu, G., Cai, W., 2014. Wet Etching-Assisted Colloidal Lithography: A General Strategy toward Nanodisk and Nanohole Arrays on Arbitrary Substrates. ACS Appl. Mater. Interfaces 6, 9207–9213. https://doi.org/10/f58mhn

Wang, J., Munir, A., Li, Z., Zhou, H.S., 2009. Aptamer–Au NPs conjugates-enhanced SPR sensing for the ultrasensitive sandwich immunoassay. Biosens. Bioelectron. 25, 124–129. https://doi.org/10.1016/j.bios.2009.06.016

Wang, L., Song, Q., Liu, Q., He, D., Ouyang, J., 2015. Plasmon-Enhanced Fluorescence-Based Core-Shell Gold Nanorods as a Near-IR Fluorescent Turn-On Sensor for the Highly Sensitive Detection of Pyrophosphate in Aqueous Solution. Adv. Funct. Mater. 25, 7017–

7027. https://doi.org/10.1002/adfm.201503326

Wang, S., Esfahani, M., Gurkan, U.A., Inci, F., Kuritzkes, D.R., Demirci, U., 2012. Efficient on-chip isolation of HIV subtypes. Lab. Chip 12, 1508. https://doi.org/10.1039/c2lc20706k

Wang, X., Chang, T.-W., Lin, G., Gartia, M.R., Liu, G.L., 2017. Self-Referenced Smartphone-Based Nanoplasmonic Imaging Platform for Colorimetric Biochemical Sensing. Anal. Chem. 89, 611–615. https://doi.org/10.1021/acs.analchem.6b02484

Wang, X., Zhu, J., Tong, H., Yang, X., Wu, X., Pang, Z., Yang, H., Qi, Y., 2019. A theoretical study of a plasmonic sensor comprising a gold nano-disk array on gold film with a SiO_2 spacer. Chin. Phys. B 28, 044201. https://doi.org/10.1088/1674-1056/28/4/044201

Wei, W., Nong, J., Zhang, G., Zhu, Y., 2014. An infrared biosensor based on graphene plasmonic for integrated nanofluidic analysis, in: Zhu, X., Kawata, S., Bergman, D.J., Nordlander, P., García de Abajo, F.J. (Eds.), . Presented at the SPIE/COS Photonics Asia, Beijing, China, p. 92780F. https://doi.org/10.1117/12.2071778

Weigel, A., Sebesta, A., Kukura, P., n.d. Dark Field Micro-Spectroscopy with Single-Molecule Fluorescence Sensitivity. ACS Photonics 11.

Willets, K.A., Van Duyne, R.P., 2007. Localized Surface Plasmon Resonance Spectroscopy and Sensing. Annu. Rev. Phys. Chem. 58, 267–297. https://doi.org/10/b5zpjb

Woessner, A., Lundeberg, M.B., Gao, Y., Principi, A., Alonso-González, P., Carrega, M., Watanabe, K., Taniguchi, T., Vignale, G., Polini, M., Hone, J., Hillenbrand, R., Koppens, F.H.L., 2015a. Highly confined low-loss plasmons in graphene–boron nitride heterostructures. Nat. Mater. 14, 421–425. https://doi.org/10.1038/nmat4169

Woessner, A., Lundeberg, M.B., Gao, Y., Principi, A., Alonso-González, P., Carrega, M., Watanabe, K., Taniguchi, T., Vignale, G., Polini, M., Hone, J., Hillenbrand, R., Koppens, F.H.L., 2015b. Highly confined low-loss plasmons in graphene–boron nitride heterostructures. Nat. Mater. 14, 421–425. https://doi.org/10/gfwst6

Wu, C., Khanikaev, A.B., Adato, R., Arju, N., Yanik, A.A., Altug, H., Shvets, G., 2012. Fano-resonant asymmetric metamaterials for ultrasensitive spectroscopy and identification of molecular monolayers. Nat. Mater. 11, 69–75. https://doi.org/10.1038/nmat3161

Xianyu, Y., Chen, Y., Jiang, X., 2015. Horseradish Peroxidase-Mediated, Iodide-Catalyzed Cascade Reaction for Plasmonic Immunoassays. Anal. Chem. 87, 10688–10692. https://doi.org/10.1021/acs.analchem.5b03522

Xiao, S., Wang, T., Liu, Y., Han, X., Yan, X., 2017. An Ultrasensitive and Multispectral Refractive Index Sensor Design Based on Quad-Supercell Metamaterials. Plasmonics 12, 185–191. https://doi.org/10.1007/s11468-016-0248-8

Yanik, A.A., Cetin, A.E., Huang, M., Artar, A., Mousavi, S.H., Khanikaev, A., Connor, J.H., Shvets, G., Altug, H., 2011. Seeing protein monolayers with naked eye through plasmonic Fano resonances. Proc. Natl. Acad. Sci. 108, 11784–11789. https://doi.org/10.1073/pnas.1101910108

Yockell-Lelièvre, H., Lussier, F., Masson, J.-F., 2015. Influence of the Particle Shape and Density of Self-Assembled Gold Nanoparticle Sensors on LSPR and SERS. J. Phys. Chem. C 119, 28577–28585. https://doi.org/10.1021/acs.jpcc.5b09570

Yuan, H., Liu, Y., Fales, A.M., Li, Y.L., Liu, J., Vo-Dinh, T., 2013. Quantitative Surface-Enhanced Resonant Raman Scattering Multiplexing of Biocompatible Gold Nanostars for in Vitro and ex Vivo Detection. Anal. Chem. 85, 208–212. https://doi.org/10.1021/ac302510g

Yuan, J., Oliver, R., Li, J., Lee, J., Aguilar, M., Wu, Y., 2007. Sensitivity enhancement of SPR assay of progesterone based on mixed self-assembled monolayers using nanogold particles. Biosens. Bioelectron. 23, 144–148. https://doi.org/10.1016/j.bios.2007.03.025

Zhang, D., Wang, K., Wei, W., Liu, S., 2020. Single-Particle Assay of Poly(ADP-ribose) Polymerase-1 Activity with Dark-Field Optical Microscopy. ACS Sens. 9.

Zhang, Q., Yu, Y., Yun, X., Luo, B., Jiang, H., Chen, C., Wang, S., Min, D., 2020. Multicolor Colorimetric Sensor for Detection of Omethoate Based on the Inhibition of the Enzyme-Induced Metallization of Gold Nanorods. ACS Appl. Nano Mater. 3, 5212–5219. https://doi.org/10.1021/acsanm.0c00641

Zhang, W., Ma, H., Fan, J., 2019. Scaling Relations of Plasmon Resonance Peak in Au@Fe3O4 Core-Shell Nanohybrids Structure. Plasmonics 14, 1123–1129. https://doi.org/10.1007/s11468-018-00901-w

Zhang, X., Xie, Y., 2013. Recent advances in free-standing two-dimensional crystals with atomic thickness: design, assembly and transfer strategies. Chem. Soc. Rev. 42, 8187. https://doi.org/10.1039/c3cs60138b

Zhang, Z., Yang, M., Yan, X., Guo, X., Li, J., Yang, Y., Wei, D., Liu, L., Xie, J., Liu, Y., Liang, L., Yao, J., 2020. The Antibody-Free Recognition of Cancer Cells Using Plasmonic Biosensor Platforms with the Anisotropic Resonant Metasurfaces. ACS Appl. Mater. Interfaces 12, 11388–11396. https://doi.org/10.1021/acsami.0c00095

Zhao, Y., Hu, X., Chen, G., Zhang, X., Tan, Z., Chen, J., Ruoff, R.S., Zhu, Y., Lu, Y., 2013a. Infrared biosensors based on graphene plasmonics: modeling. Phys. Chem. Chem. Phys. 15, 17118. https://doi.org/10/ghbtq8

Zhao, Y., Hu, X., Chen, G., Zhang, X., Tan, Z., Chen, J., Ruoff, R.S., Zhu, Y., Lu, Y., 2013b. Infrared biosensors based on graphene plasmonics: modeling. Phys. Chem. Chem. Phys. 15, 17118. https://doi.org/10.1039/c3cp51952j

Zheng, W., Jiang, X., 2016. Integration of nanomaterials for colorimetric immunoassays with improved performance: a functional perspective. The Analyst 141, 1196–1208. https://doi.org/10.1039/C5AN02222C

Zhou, P., Zheng, G., 2018. High-efficient light absorption of monolayer graphene via cylindrical dielectric arrays and the sensing application. Opt. Mater. 78, 471–476. https://doi.org/10.1016/j.optmat.2018.02.060

Zhu, J., Wang, Z., Lin, S., Jiang, S., Liu, X., Guo, S., 2020. Low-cost flexible plasmonic nanobump metasurfaces for label-free sensing of serum tumor marker. Biosens. Bioelectron. 150, 111905. https://doi.org/10.1016/j.bios.2019.111905

Zijlstra, P., Orrit, M., 2011. Single metal nanoparticles. Rep Prog Phys 56.

Highlights

For

Strategies to Improve Performances of LSPR Biosensing: Structure, Materials and Interface Modification

Tianping Xu[a] and Zhaoxin Geng[a, b*]

[a] School of Information Engineering, Minzu University of China, Beijing, 100081, P. R. China
[b] State Key Laboratory for Integrated Optoelectronics, Institute of Semiconductors, Chinese Academy of Sciences, Beijing, 100083, P. R. China

*Corresponding author.
E-mail addresses: zxgeng@muc.edu.cn (Z. Geng).

The sensing and detection technology based on Localized Surface Plasmon Resonance (LSPR) develops rapidly. However, it has not been popularized in clinical application, which is mainly due to the low sensitivity, low repeatability and low reliability of LSPR sensor. Although there are many literatures summarizing the work of LSPR, LSPR has attracted the attention and research of many scholars due to its unique properties. In our years of research, we have found that three aspects are important factors for studying the clinical application of LSPR biosensors. Therefore, several aspects of LSPR sensitization (structure, material, surface modification, and the proceeding methods of LSPR biosensor) are systematically analyzed in this paper. A comprehensive analysis of the achievements in enhancing the sensitivity of LSPR biosensor is mainly reflected in the following highlights:

1. The sensing mechanism to enhance sensitivity of LSPR sensor under different metal nanostructures is summarized and the array nanostructures that can improve the repeatability of LSPR sensor are summarized. The strategy of structure sensitization is obtained.

2. The different materials (metal, 2D materials & transition metal dichalcogenides (TMDs)) or structure work in different principles such as LC resonance mode, dipole resonance mode, electromagnetic induced transparency effect, Fano resonance mode, hyperbolic metamaterials, plasmonic metasurface were reviewed and the strategy to enhance sensitivity in materials was presented in detail.

3. Enhancing sensitivity by interface modification were reviewed. The perspective of LSPR biosensor integrated with microfluidics and the design with help of Artificial intelligence were proposed.

4. The proceeding methods of the LSPR bio-sensor were review and proposed the method to improve the performances.

Declaration of interests

☒ The authors declare that they have no known competing financial interests or personal relationships that could have appeared to influence the work reported in this paper.

☐The authors declare the following financial interests/personal relationships which may be considered as potential competing interests: